

**Involvement of the Glucocorticoid Receptor in Pro-inflammatory  
Transcription Factor Inhibition by Daucane Esters from  
*Laserpitium zernyi***

Višnja Popović,<sup>\*,†,‡</sup> Jan L. Goeman,<sup>†</sup> Nadia Bougarne,<sup>‡</sup> Sven Eyckerman,<sup>§,⊥</sup> Arne Heyerick<sup>‡</sup>,  
Karolien De Bosscher,<sup>§,‡,◇</sup> and Johan Van der Eycken<sup>†,◇</sup>

<sup>†</sup>Laboratory for Organic and Bio-Organic Synthesis, Department of Organic and  
Macromolecular Chemistry, Ghent University, Krijgslaan 281 (S.4), B-9000 Ghent, Belgium

<sup>‡</sup>Receptor Research Laboratories, Nuclear Receptor Lab, VIB-UGent Center for Medical  
Biotechnology, Ghent University, Albert Baertsoenkaai 3, B-9000 Ghent, Belgium

<sup>§</sup>Department of Biochemistry, Ghent University, Albert Baertsoenkaai 3, B-9000 Ghent,  
Belgium

<sup>⊥</sup>VIB-UGent Center for Medical Biotechnology, Ghent University, Albert Baertsoenkaai 3, B-  
9000 Ghent, Belgium

<sup>‡</sup>Reliable Cancer Therapies, Boechoutlaan 221, B-1853 Strombeek-Bever, Belgium

<sup>◇</sup>Shared senior authorship

\* Corresponding author (V. Popović) at: Ghent University - Faculty of Sciences, Department of Organic and  
Macromolecular Chemistry, Krijgslaan 281, S4, 9 000 Ghent, Belgium. Tel.: +32 9264 4476; Fax: +32 9264  
4998. E-mail address: [Visnja.Popovic@vib-ugent.be](mailto:Visnja.Popovic@vib-ugent.be)

**Supporting Information**

Table of contents:

S1. <sup>1</sup>H NMR spectrum of the new compound **1** (500 MHz) in CDCl<sub>3</sub>.

S2. APT spectrum of the new compound **1** (125 MHz) in CDCl<sub>3</sub>.

S3. COSY spectrum the new compound **1** in CDCl<sub>3</sub>.

S4. HSQC spectrum of the new compound **1** in CDCl<sub>3</sub>.

S5. HMBC spectrum of the new compound **1** in CDCl<sub>3</sub>.

S6. NOESY spectrum of the new compound **1** in CDCl<sub>3</sub>.

S7. HR-MS spectrum of the new compound **1**.

S8. LC-MS data of the new compound **1**.

S9. IR spectrum of the new compound **1**.

S10. <sup>1</sup>H NMR spectrum of the new compound **2** (300 MHz) in CDCl<sub>3</sub>.

S11. APT spectrum of the new compound **2** (75 MHz) in CDCl<sub>3</sub>.

S12. COSY spectrum the new compound **2** in CDCl<sub>3</sub>.

S13. HSQC spectrum of the new compound **2** in CDCl<sub>3</sub>.

S14. HMBC spectrum of the new compound **2** in CDCl<sub>3</sub>.

S15. HR-MS spectrum of the new compound **2**.

S16. LC-MS data of the new compound **2**.

S17. IR spectrum of the new compound **2**.

S18. <sup>1</sup>H NMR spectrum of the new compound **3** (500 MHz) in CDCl<sub>3</sub>.

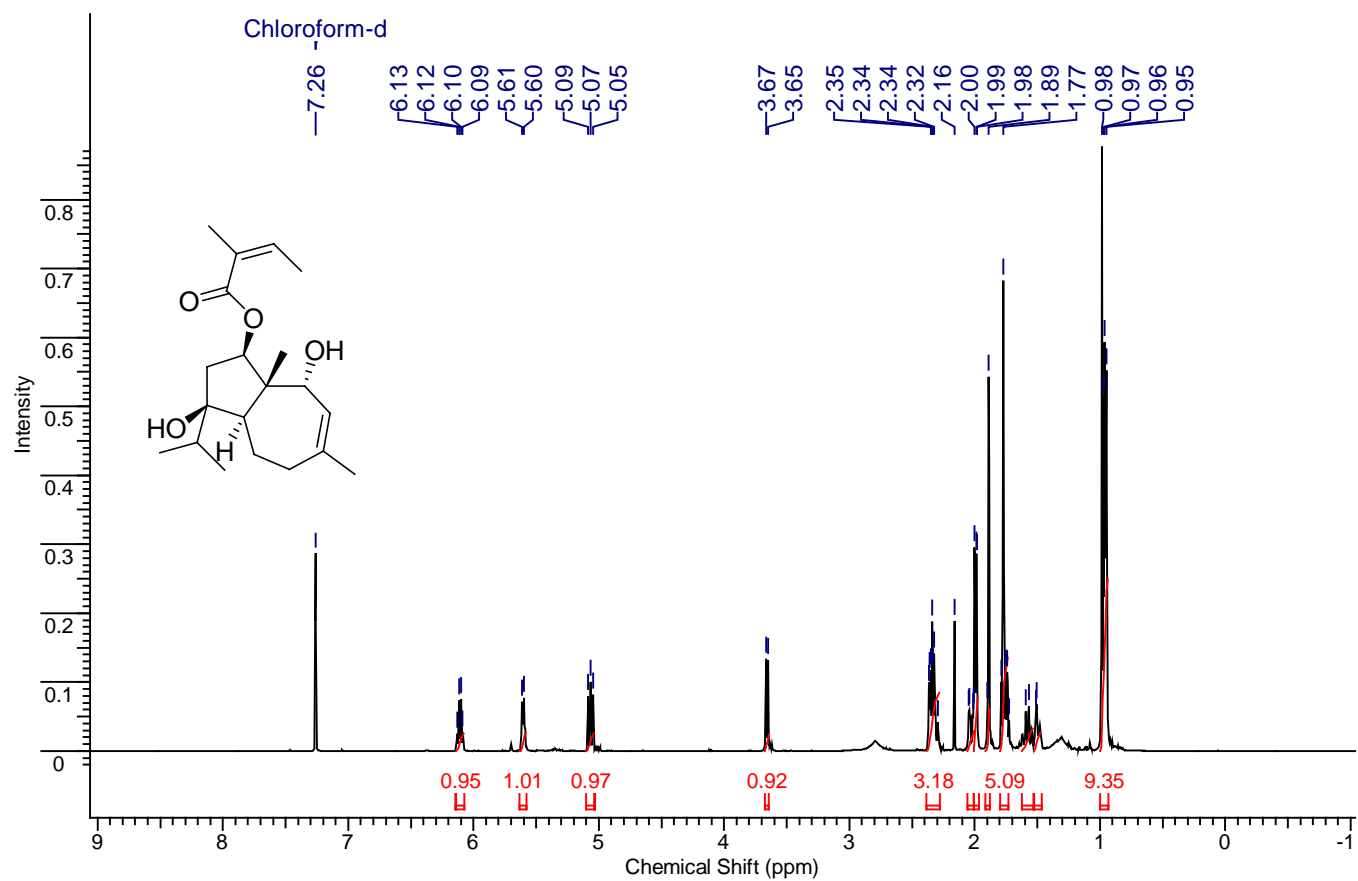
S19. APT spectrum of the new compound **3** (125 MHz) in CDCl<sub>3</sub>.

S20. COSY spectrum the new compound **3** in CDCl<sub>3</sub>.

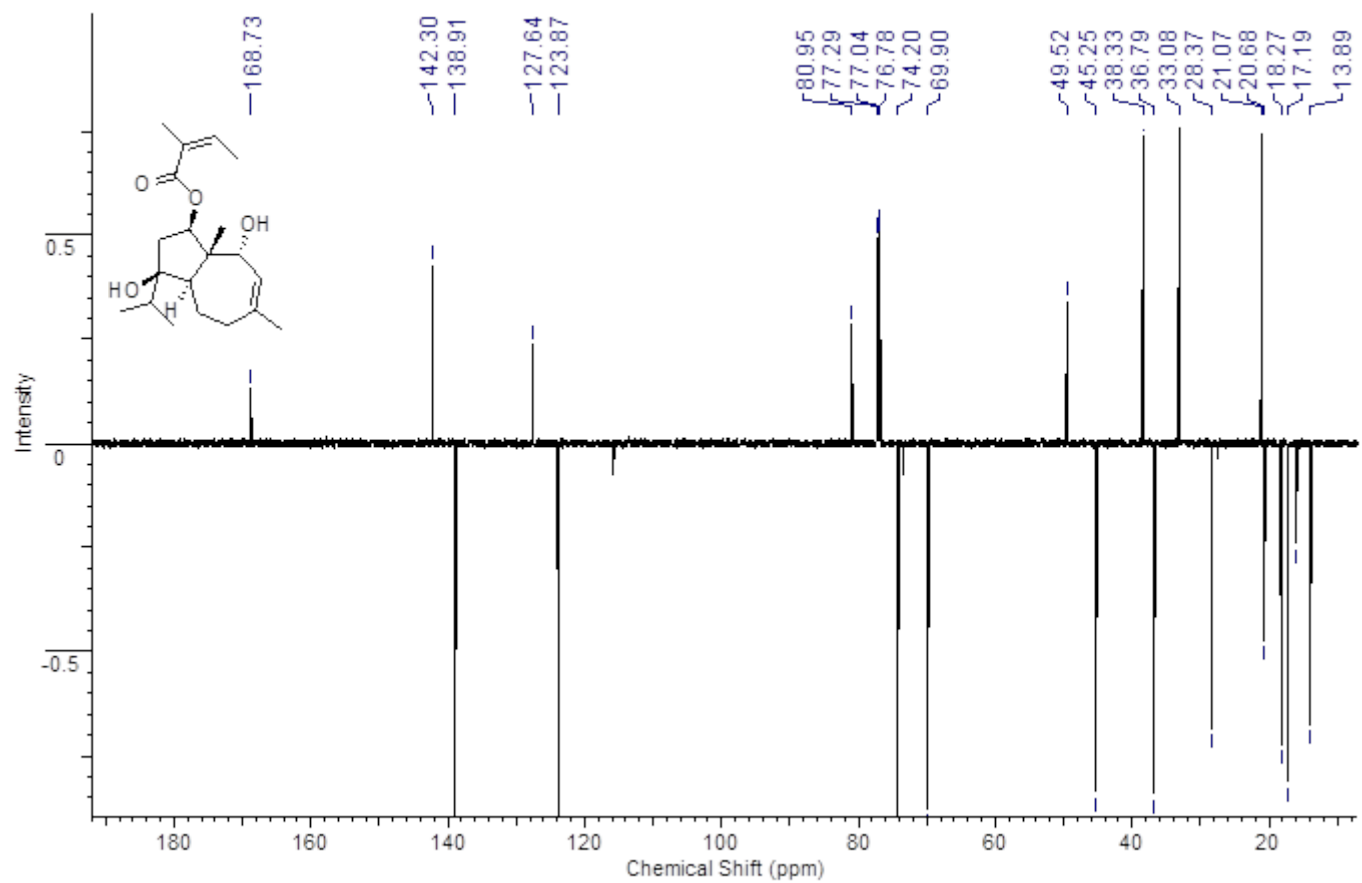
- S21. HSQC spectrum of the new compound **3** in CDCl<sub>3</sub>.
- S22. HMBC spectrum of the new compound **3** in CDCl<sub>3</sub>.
- S23. NOESY spectrum of the new compound **3** in CDCl<sub>3</sub>.
- S24. HR-MS spectrum of the new compound **3**.
- S25. LC-MS data of the new compound **3**.
- S26. IR spectrum of the new compound **3**.
- S27. <sup>1</sup>H NMR spectrum of the new compound **4** (500 MHz) in CDCl<sub>3</sub>.
- S28. APT spectrum of the new compound **4** (125 MHz) in CDCl<sub>3</sub>.
- S29. COSY spectrum the new compound **4** in CDCl<sub>3</sub>.
- S30. HSQC spectrum of the new compound **4** in CDCl<sub>3</sub>.
- S31. HMBC spectrum of the new compound **4** in CDCl<sub>3</sub>.
- S32. NOESY spectrum of the new compound **4** in CDCl<sub>3</sub>.
- S33. HR-MS spectrum of the new compound **4**.
- S34. LC-MS data of of the new compound **4**.
- S35. IR spectrum of the new compound **4**.
- S36. <sup>1</sup>H NMR spectrum of the new compound **5** (300 MHz) in CDCl<sub>3</sub>.
- S37. APT spectrum of the new compound **5** (75 MHz) in CDCl<sub>3</sub>.
- S38. COSY spectrum the new compound **5** in CDCl<sub>3</sub>.
- S39. HSQC spectrum of the new compound **5** in CDCl<sub>3</sub>.
- S40. HMBC spectrum of the new compound **5** in CDCl<sub>3</sub>.
- S41. NOESY spectrum of the new compound **5** in CDCl<sub>3</sub>.

- S42. HR-MS spectrum of the new compound **5**.
- S43. LC-MS data of of the new compound **5**.
- S44. IR spectrum of the new compound **5**.
- S45. <sup>1</sup>H NMR spectrum of the new compound **6** (500 MHz) in CDCl<sub>3</sub>.
- S46. APT spectrum of the new compound **6** (125 MHz) in CDCl<sub>3</sub>.
- S47. COSY spectrum the new compound **6** in CDCl<sub>3</sub>.
- S48. HSQC spectrum of the new compound **6** in CDCl<sub>3</sub>.
- S49. HMBC spectrum of the new compound **6** in CDCl<sub>3</sub>.
- S50. NOESY spectrum of the new compound **6** in CDCl<sub>3</sub>.
- S51. HR-MS spectrum of the new compound **6**.
- S52. LC-MS data of of the new compound **6**.
- S53. IR spectrum of the new compound **6**.
- S54. HR-MS spectrum of compound **7**.
- S55. Effect of the five most active compounds **1-3**, **7** and **8** at three concentrations (10, 30 and 60 μM) in PMA-induced A549 cells stably integrated with an AP-1-Luc-dependent reporter gene
- S56. Cell viability in κB-Luc A549 cell line as determined by the Cell Titer Glo<sup>®</sup> assay.
- S57. Cell viability in AP-1 A549 cell line as determined by the Cell Titer Glo<sup>®</sup> assay.
- S58. Cell viability in Neo Luc A549 cell line as determined in luciferase assay.
- S59. Extraction and isolation procedure.
- S60. Quantification of major components of *L. zernyi* extract
- S61. Cell cultures.

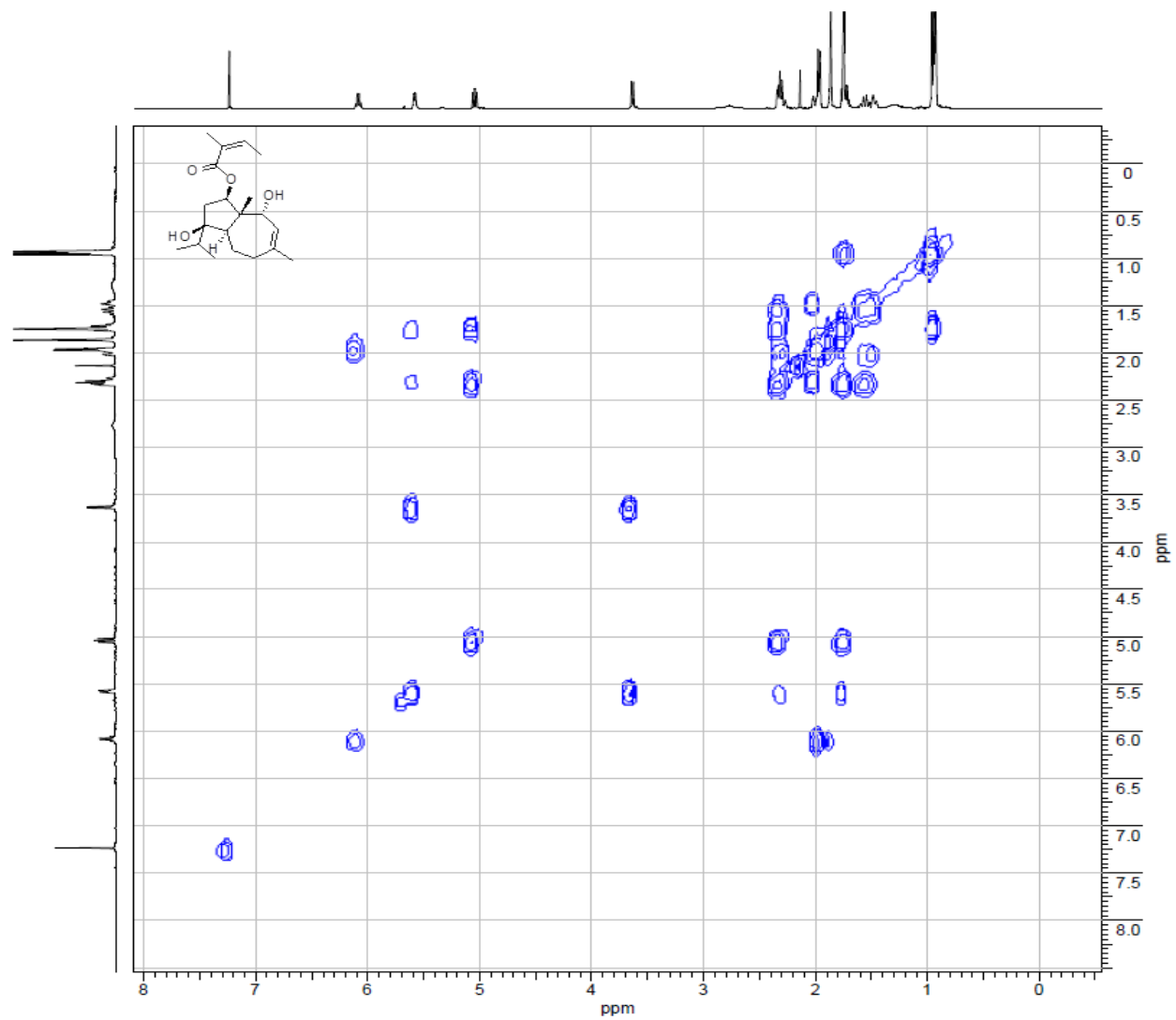
S1.  $^1\text{H}$  NMR spectrum of compound **1** (500 MHz) in  $\text{CDCl}_3$ .



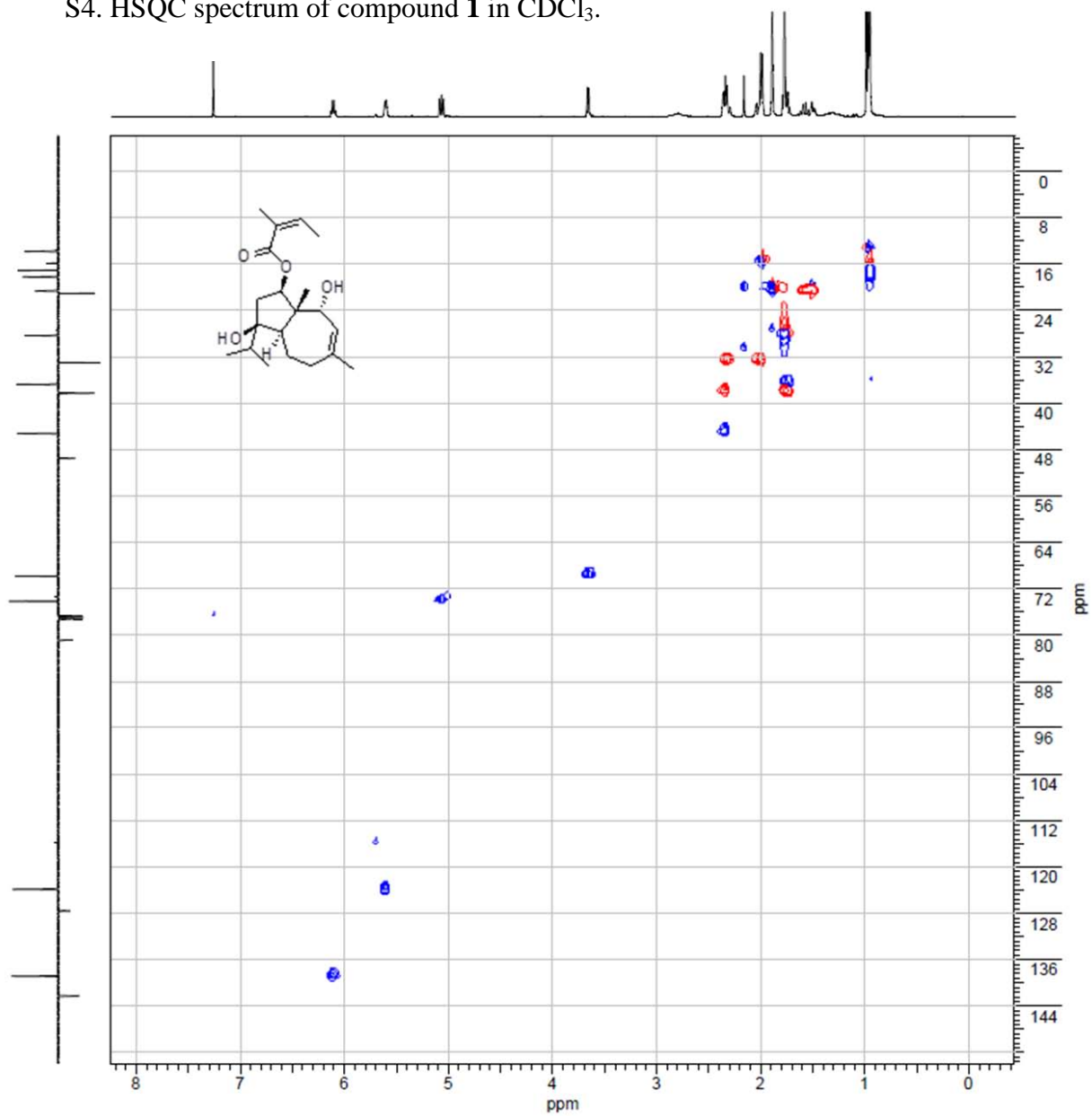
S2.  $^{13}\text{C}$  NMR spectrum of Compound **1** (125 MHz) in  $\text{CDCl}_3$ .



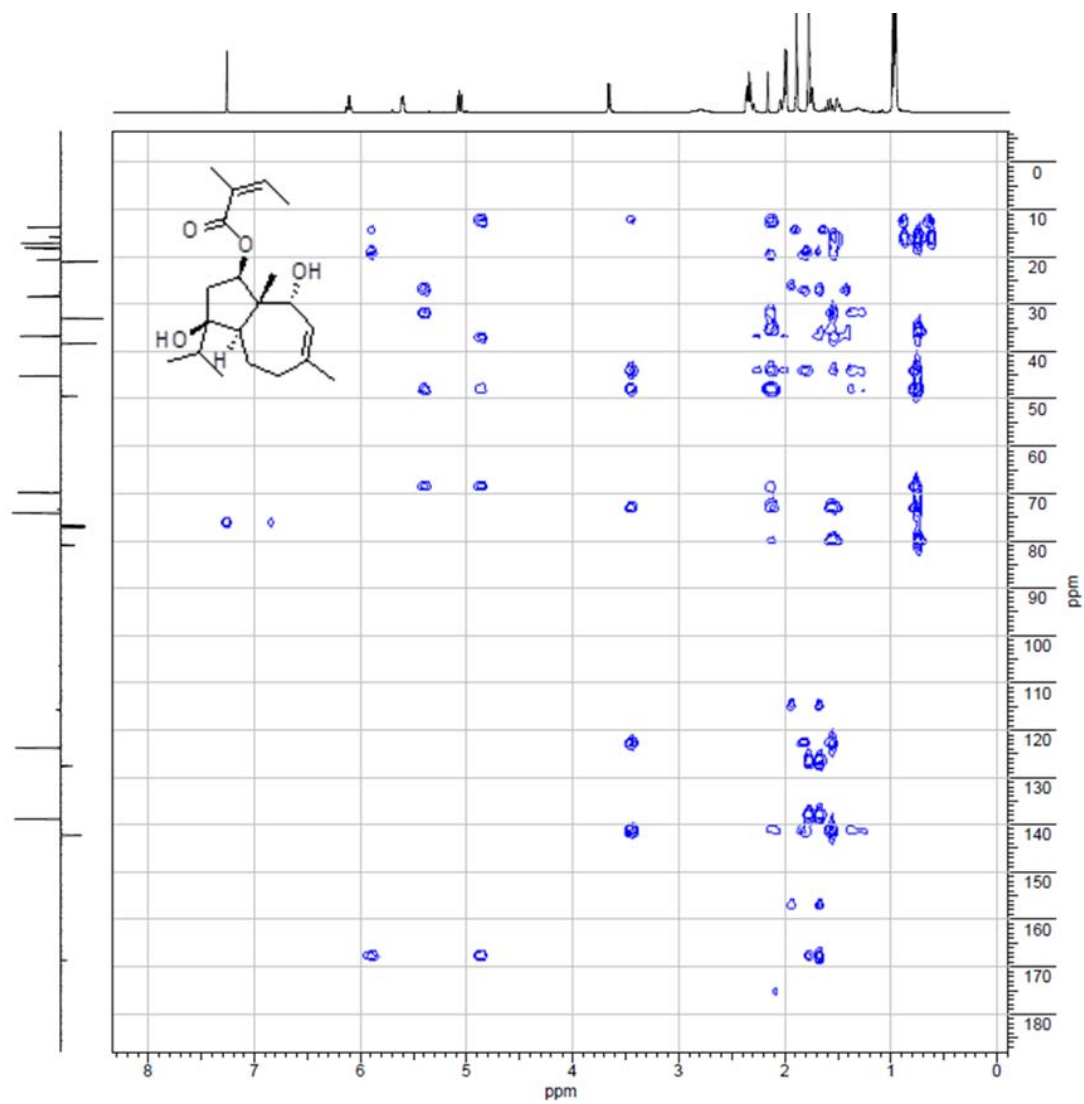
S3. COSY spectrum of compound **1** in CDCl<sub>3</sub>.



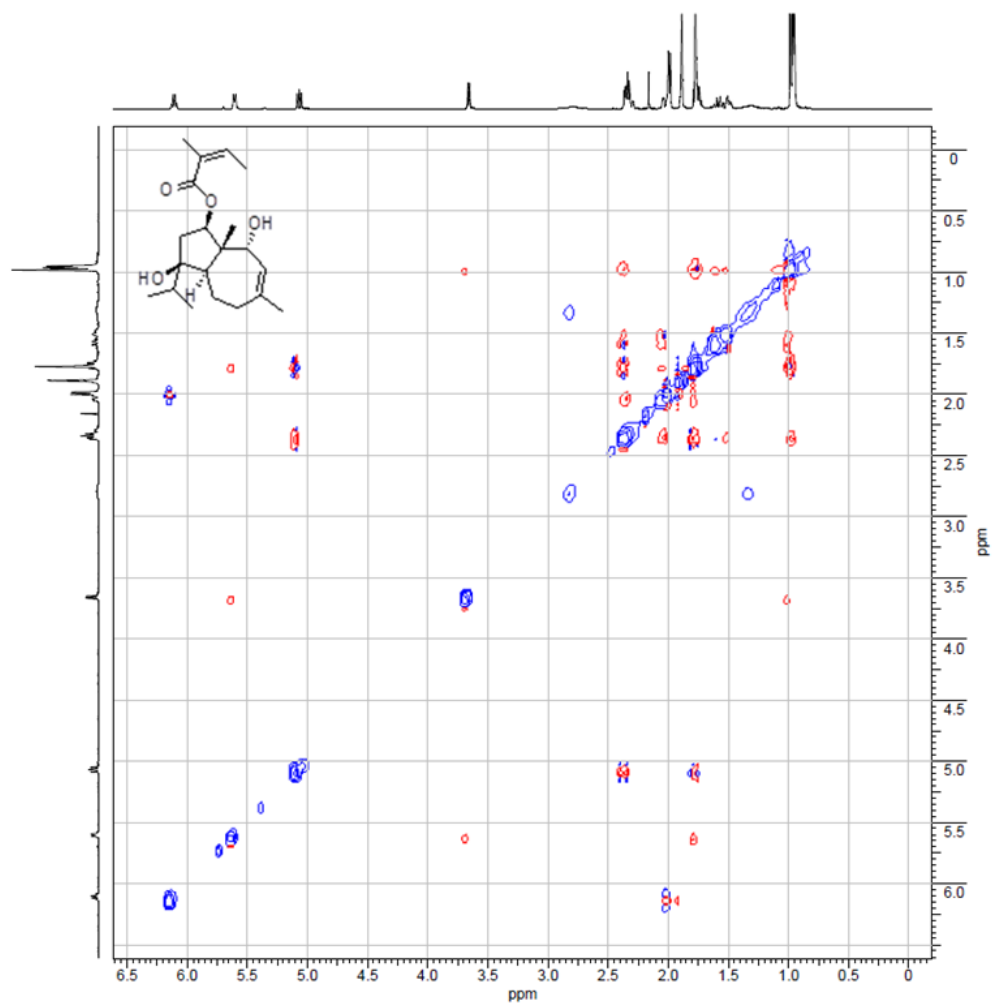
S4. HSQC spectrum of compound **1** in CDCl<sub>3</sub>.



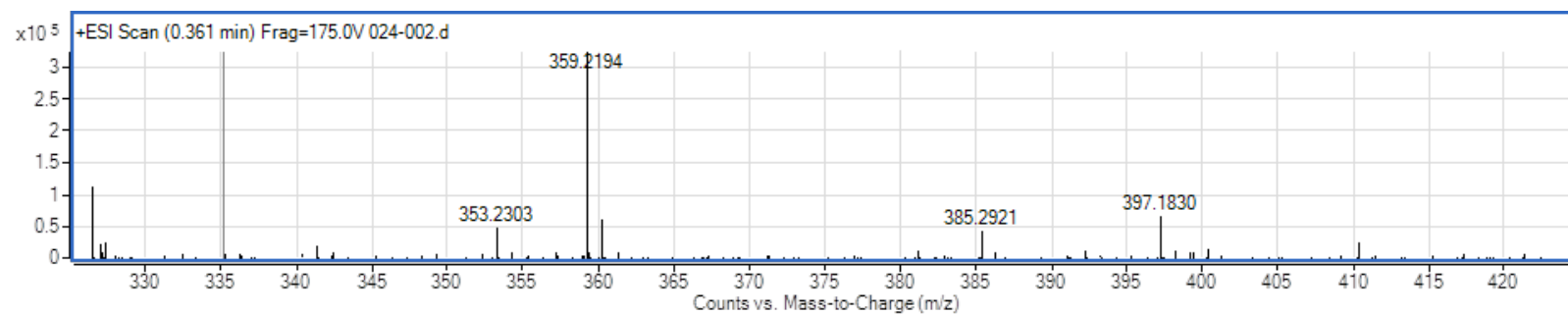
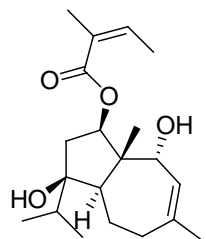
S5. HMBC spectrum of compound **1** in CDCl<sub>3</sub>.



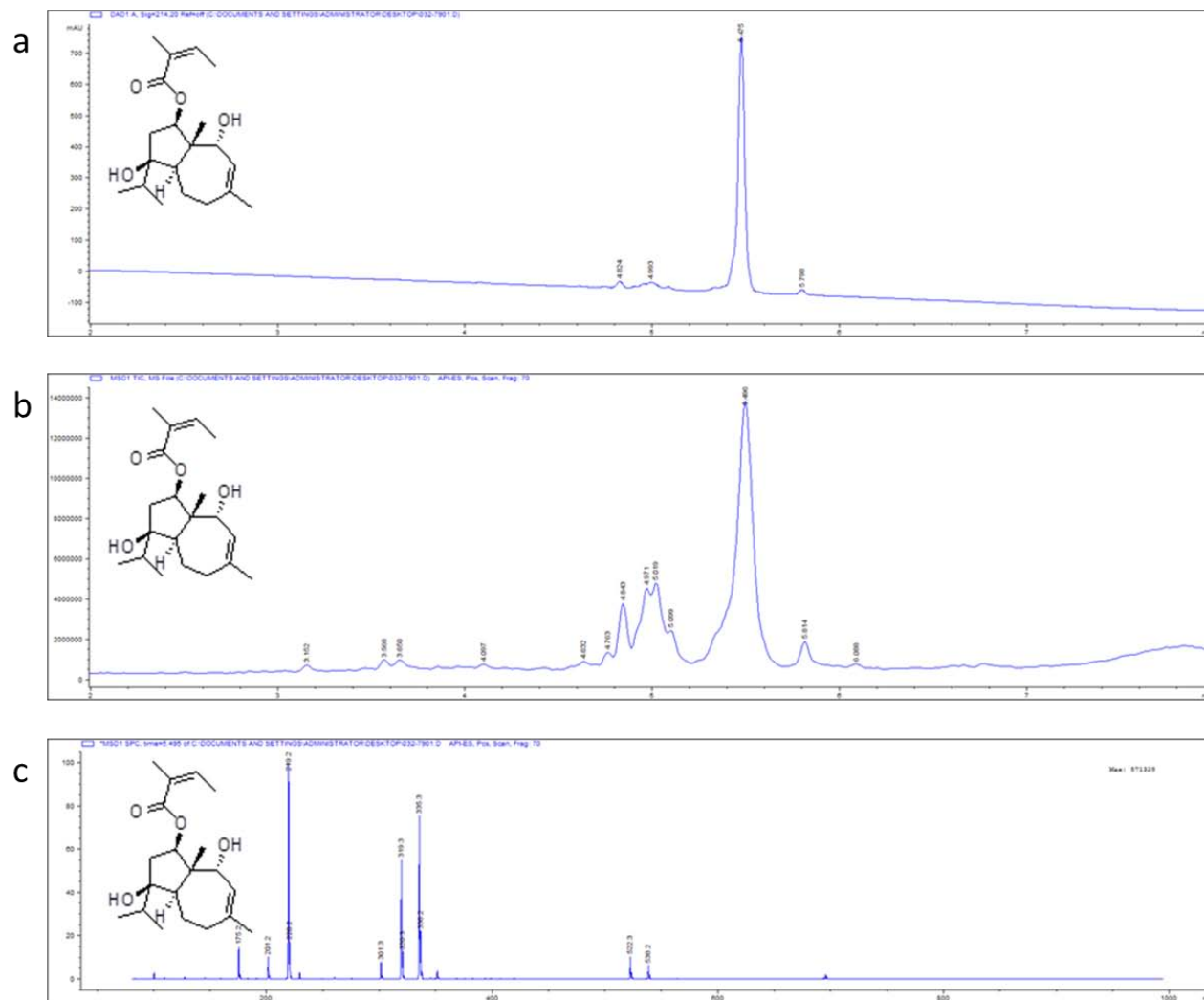
S6. NOESY spectrum of compound **1** in CDCl<sub>3</sub>.



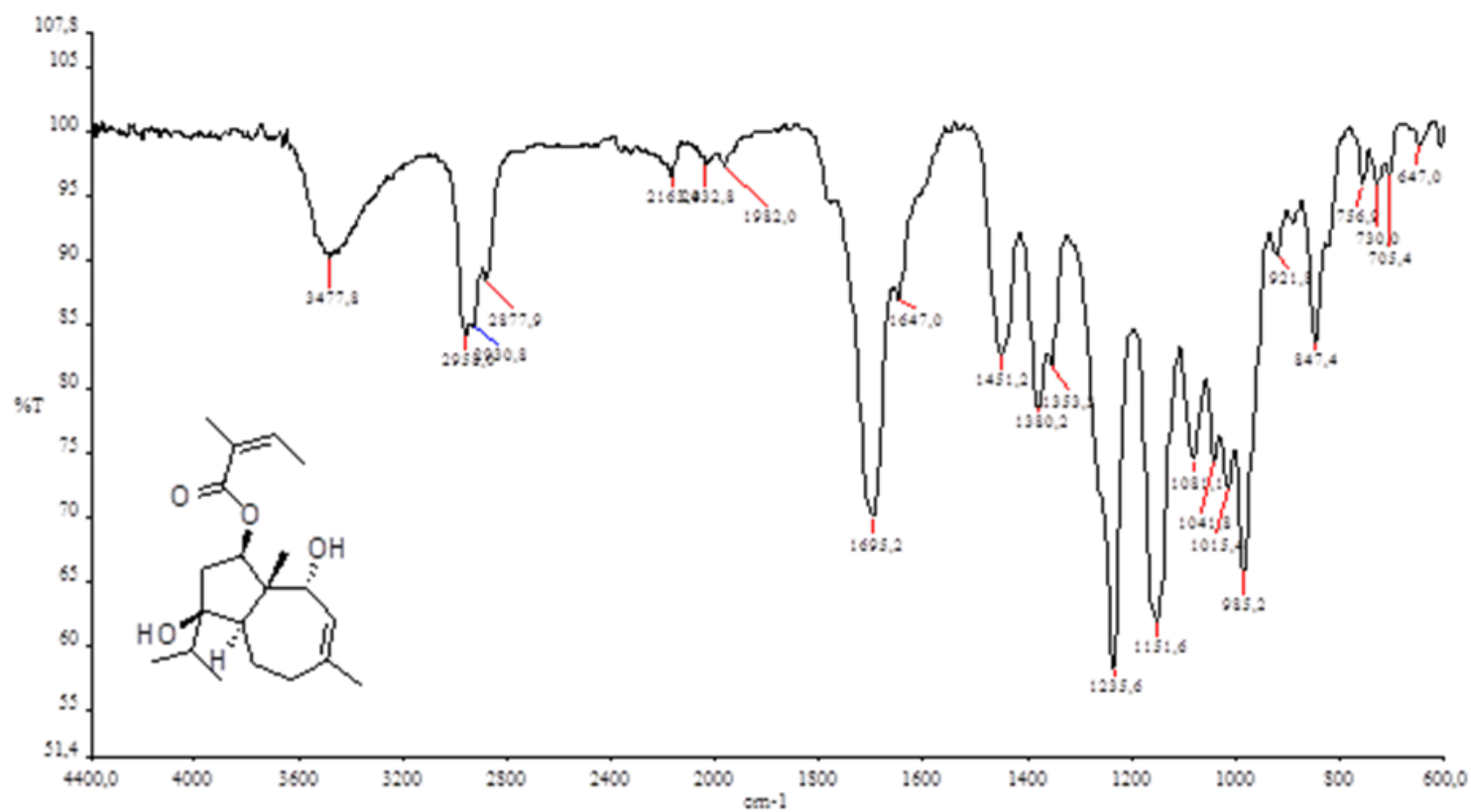
S7. HR-MS spectrum of compound **1**



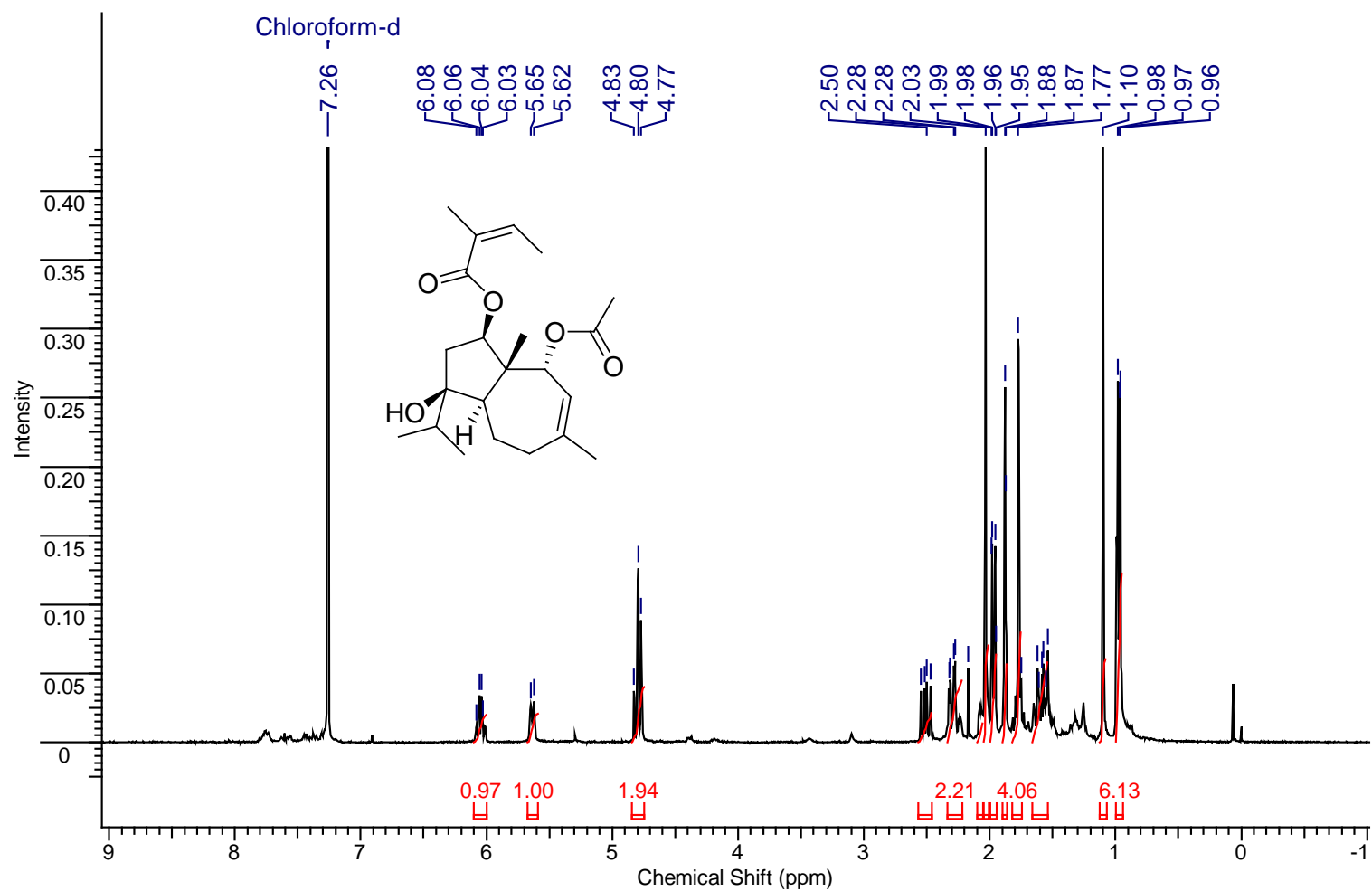
S8. LC-MS data for compound **1**. a) LC-MS chromatogram; b) Total Ion Current chromatogram; c) fragmentation spectrum of the peak of compound **1**.



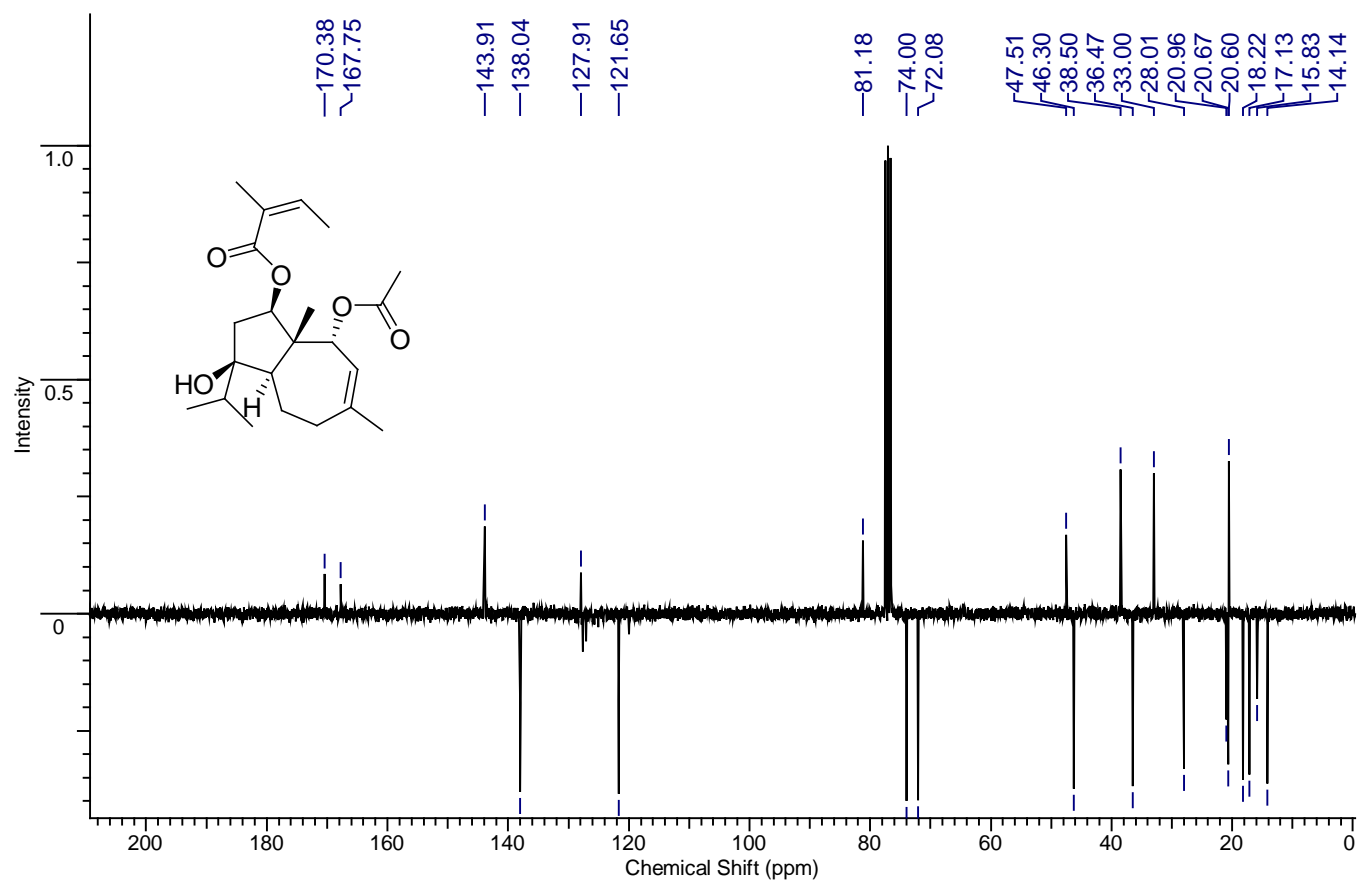
S9. IR spectrum of compound 1.



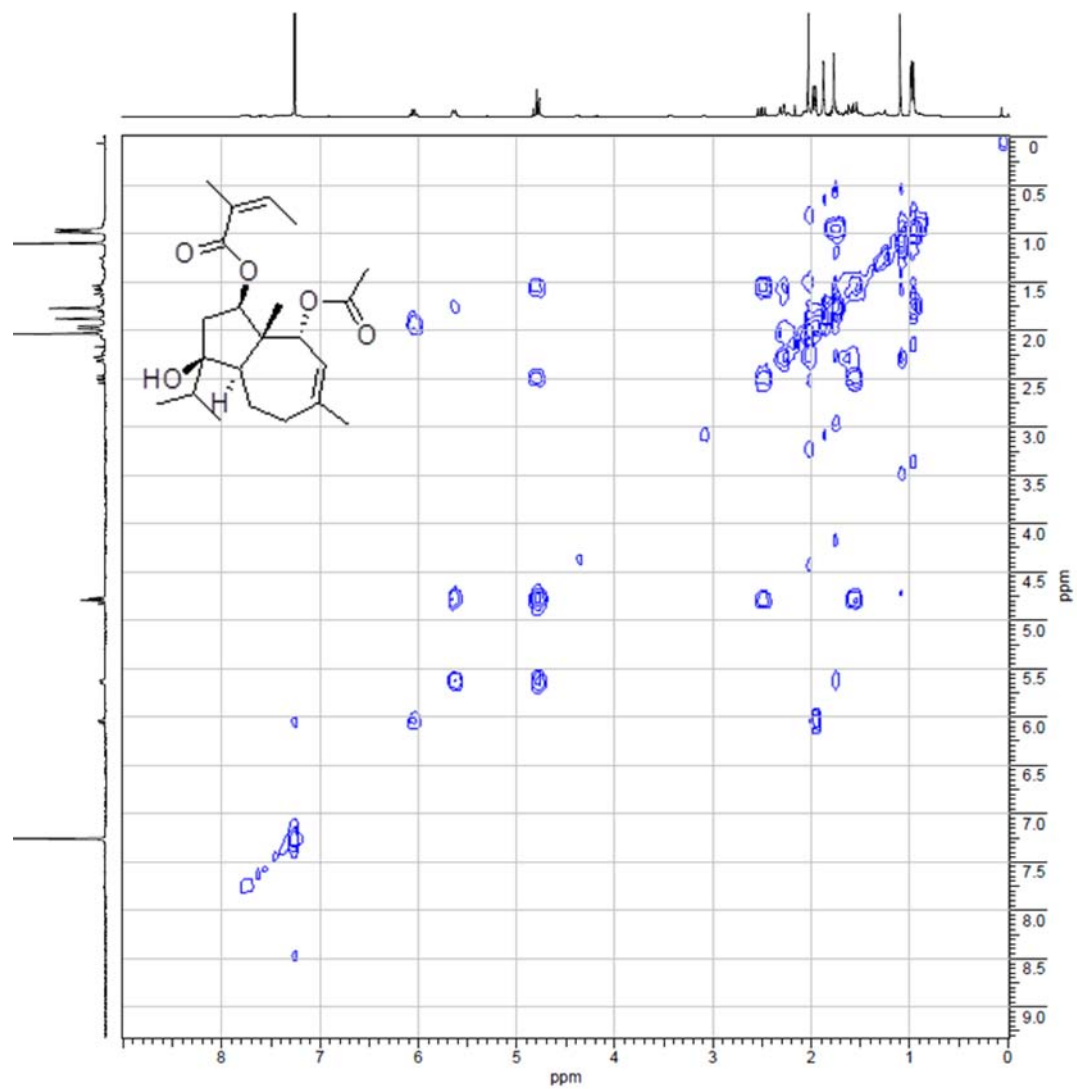
S10. <sup>1</sup>H NMR Spectrum of compound **2** (300 MHz) in CDCl<sub>3</sub>.



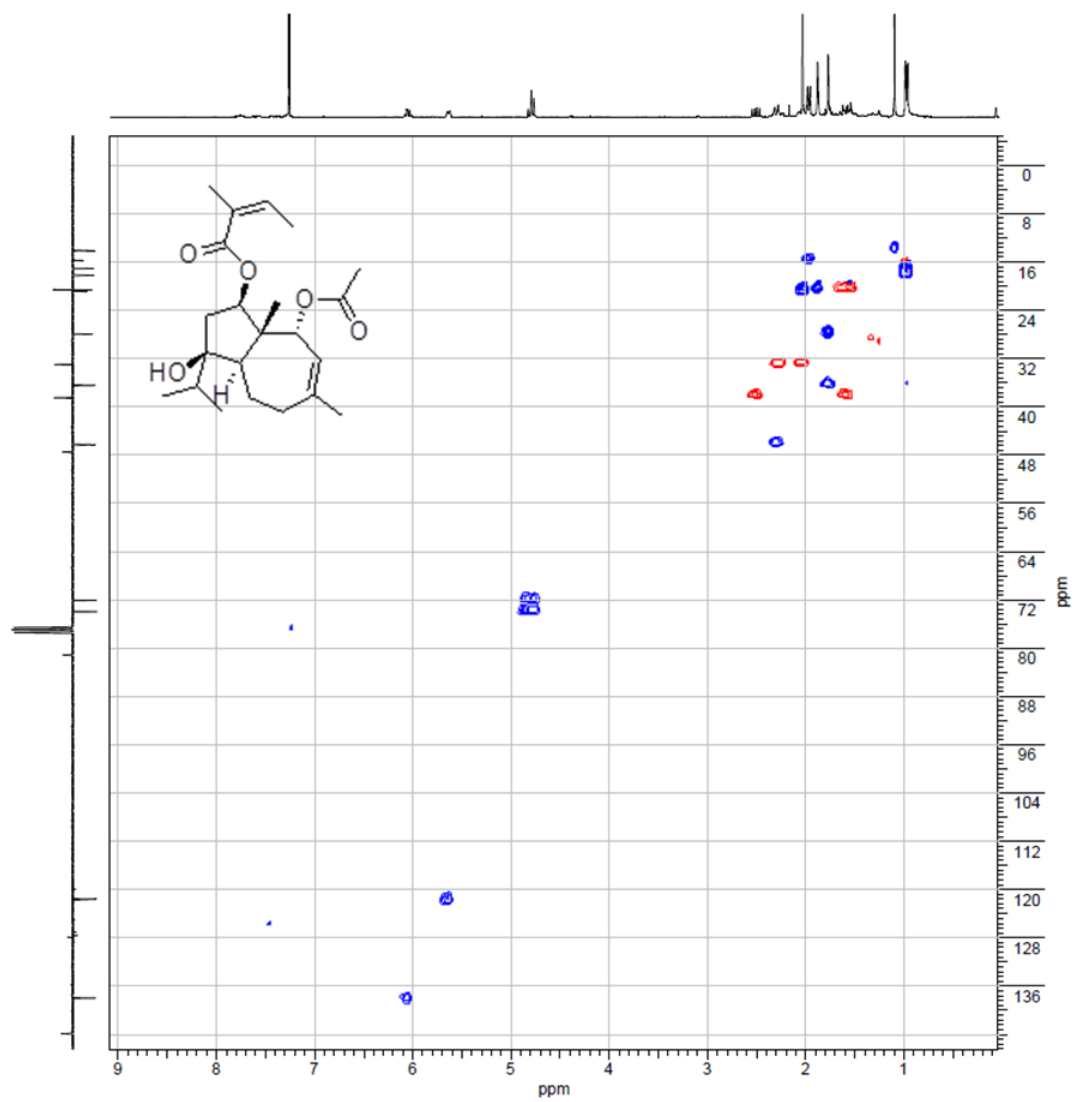
S11. APT spectrum of compound **2** (75 MHz) in CDCl<sub>3</sub>.



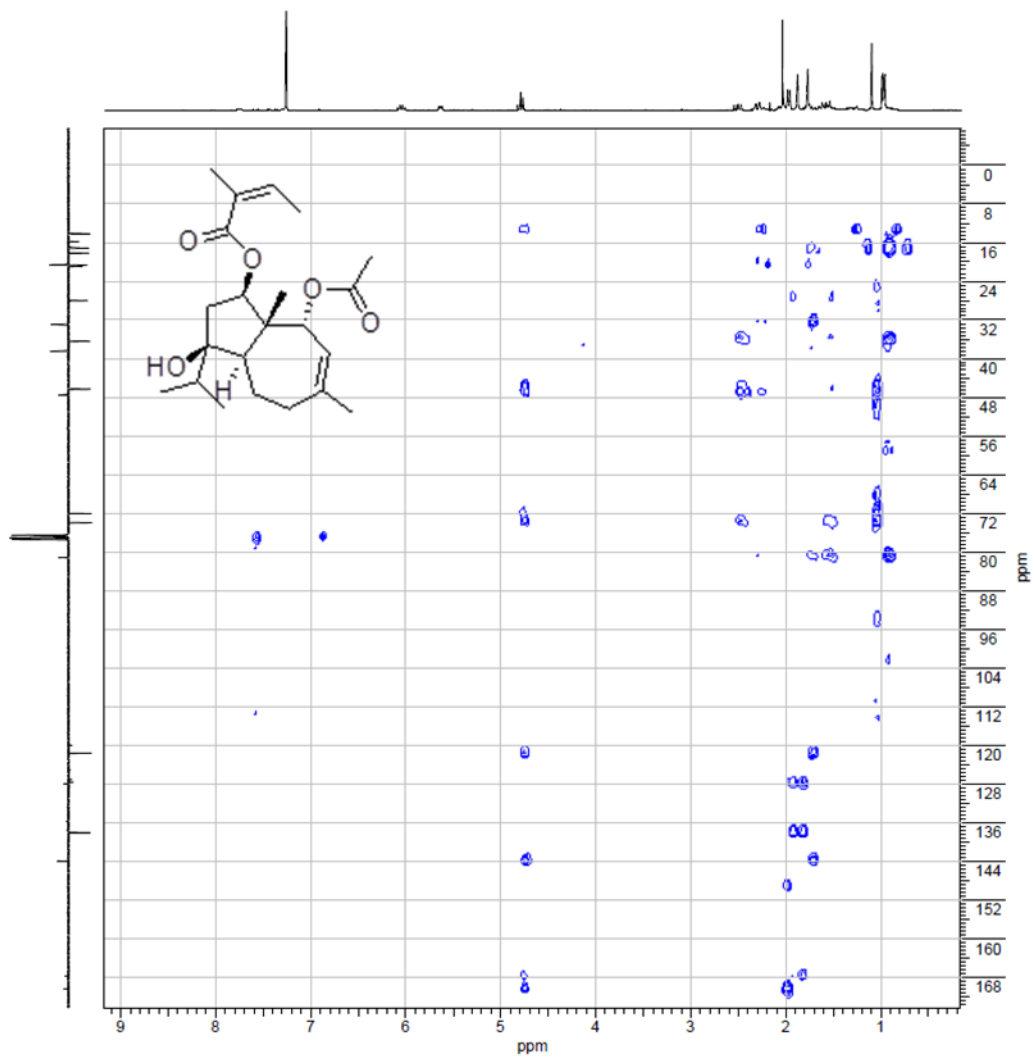
S12. COSY spectrum of compound **2** in CDCl<sub>3</sub>.



S13. HSQC spectrum of compound **2** in CDCl<sub>3</sub>.



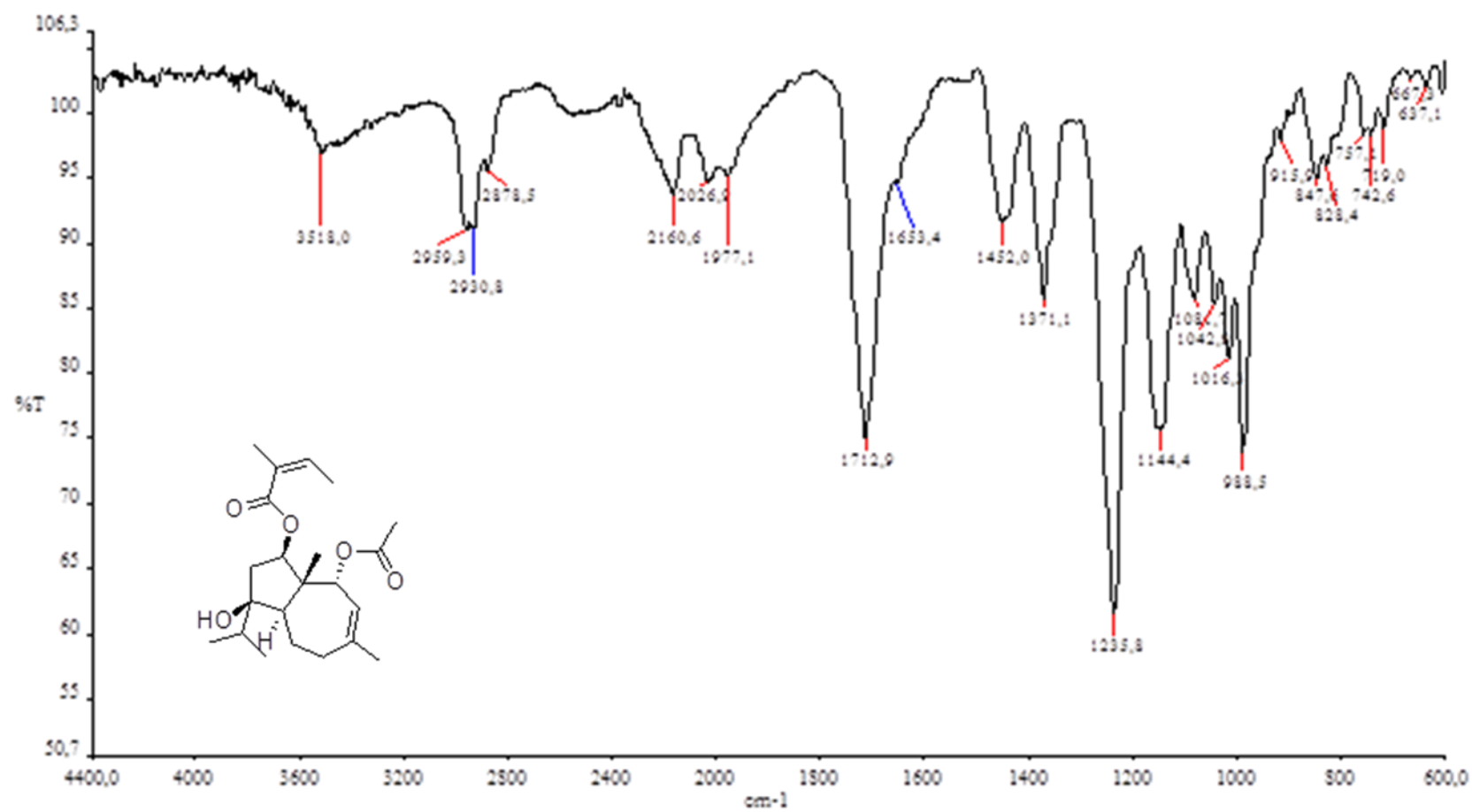
S14.HMBC spectrum of compound **2** in CDCl<sub>3</sub>.



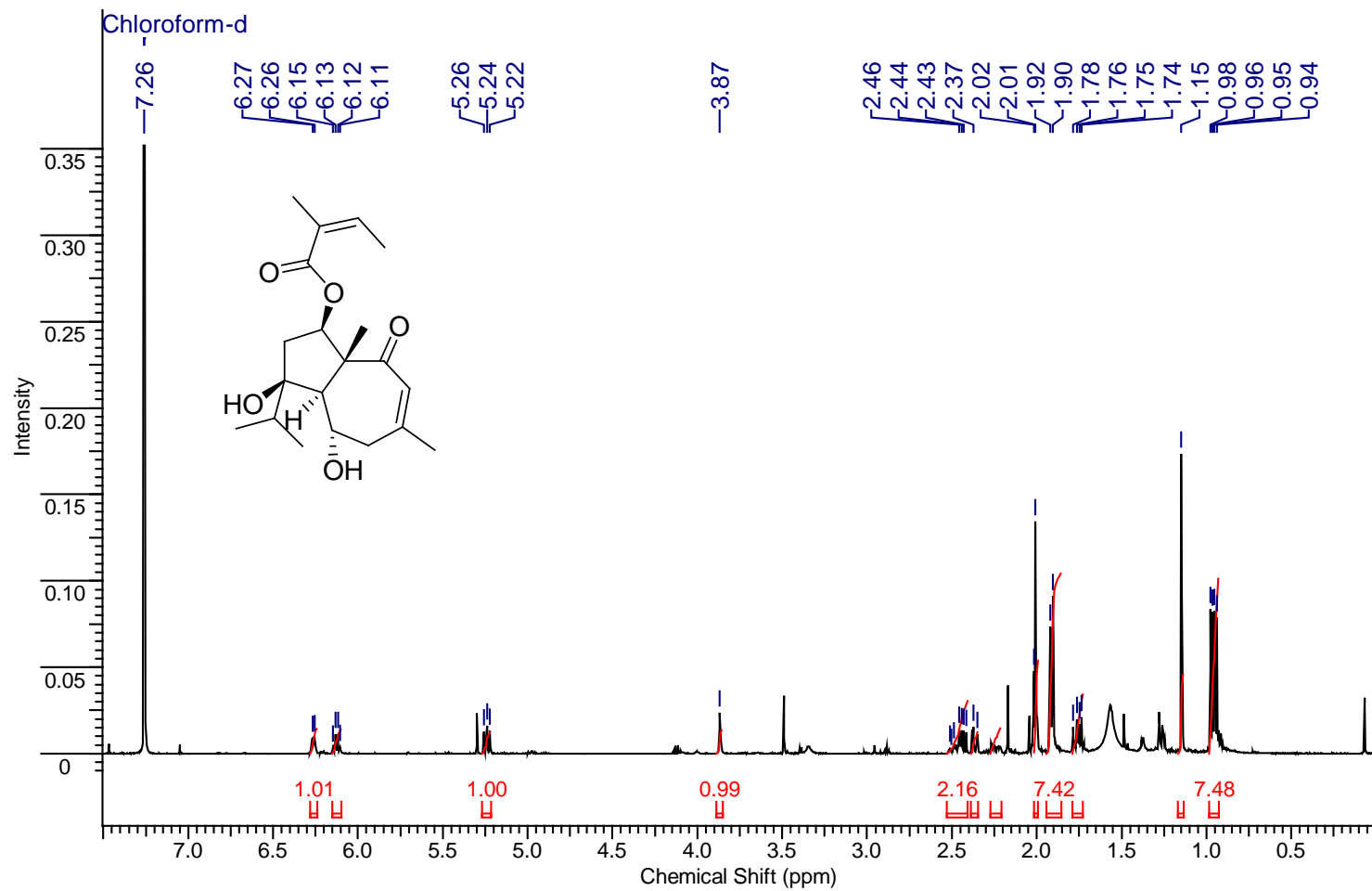




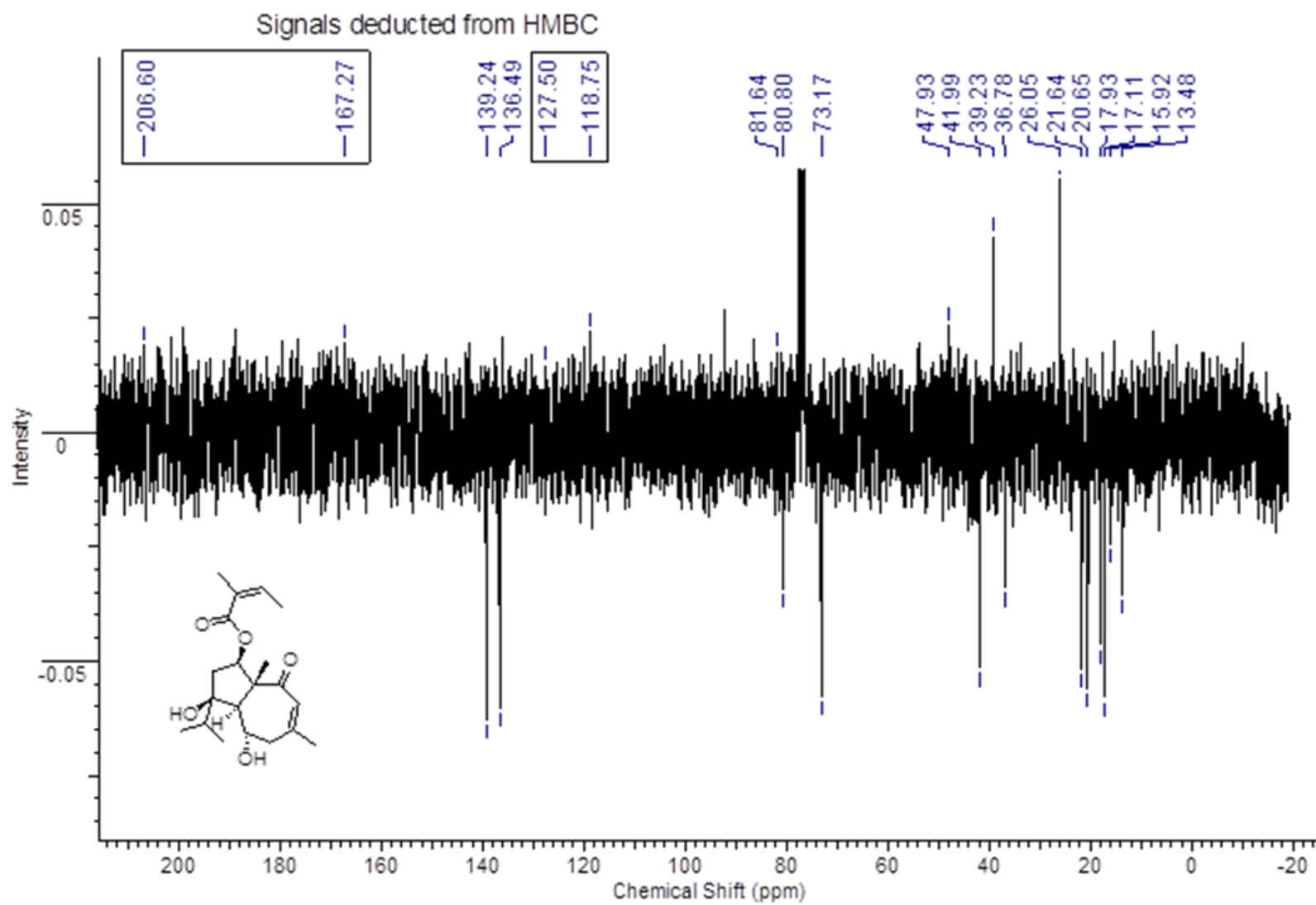
S17. IR spectrum of compound 2.



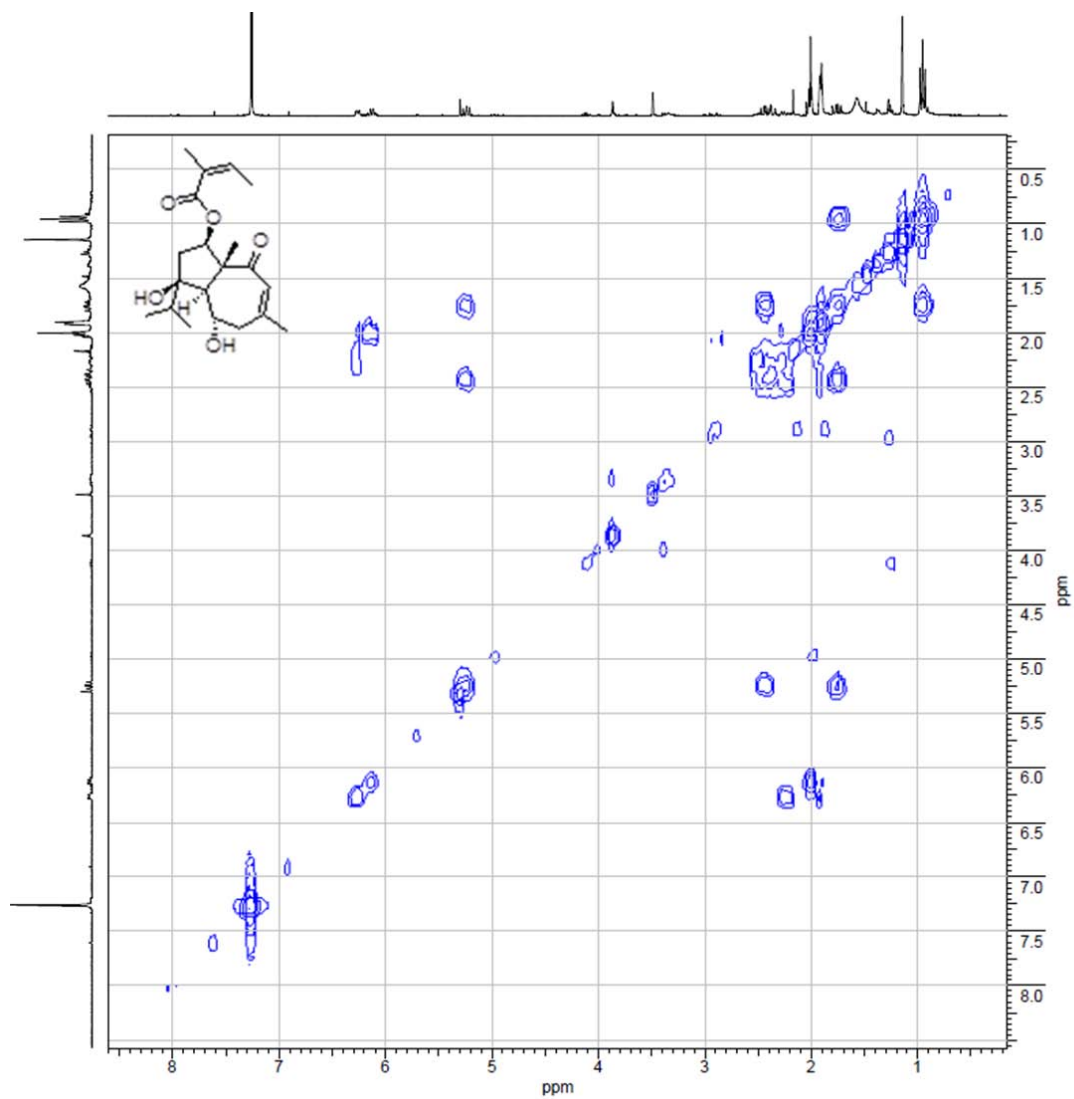
S18.  $^1\text{H}$  NMR Spectrum of compound **3** (500 MHz) in  $\text{CDCl}_3$ .



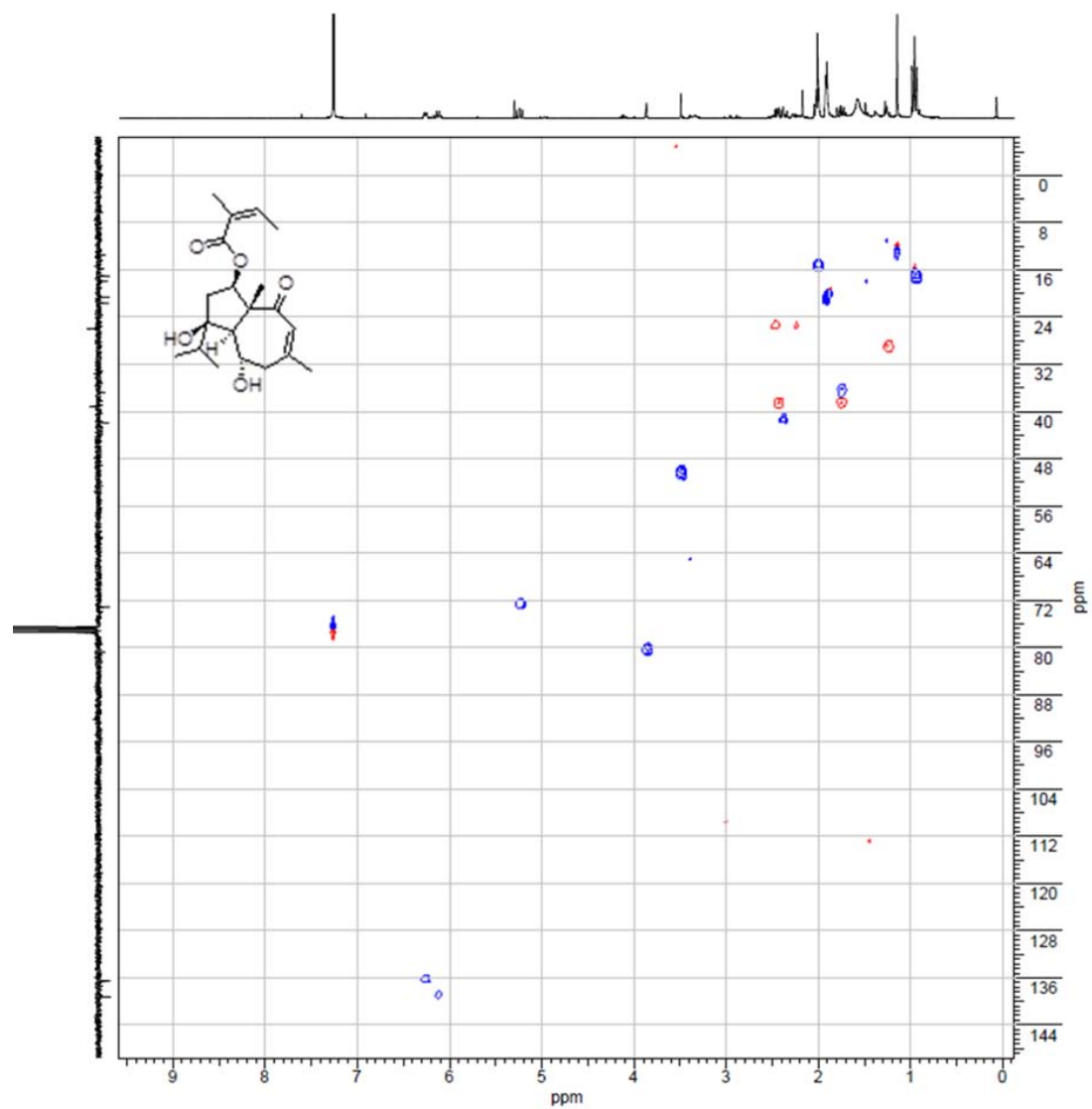
S19. APT spectrum of compound **3** (125 MHz) in CDCl<sub>3</sub>.



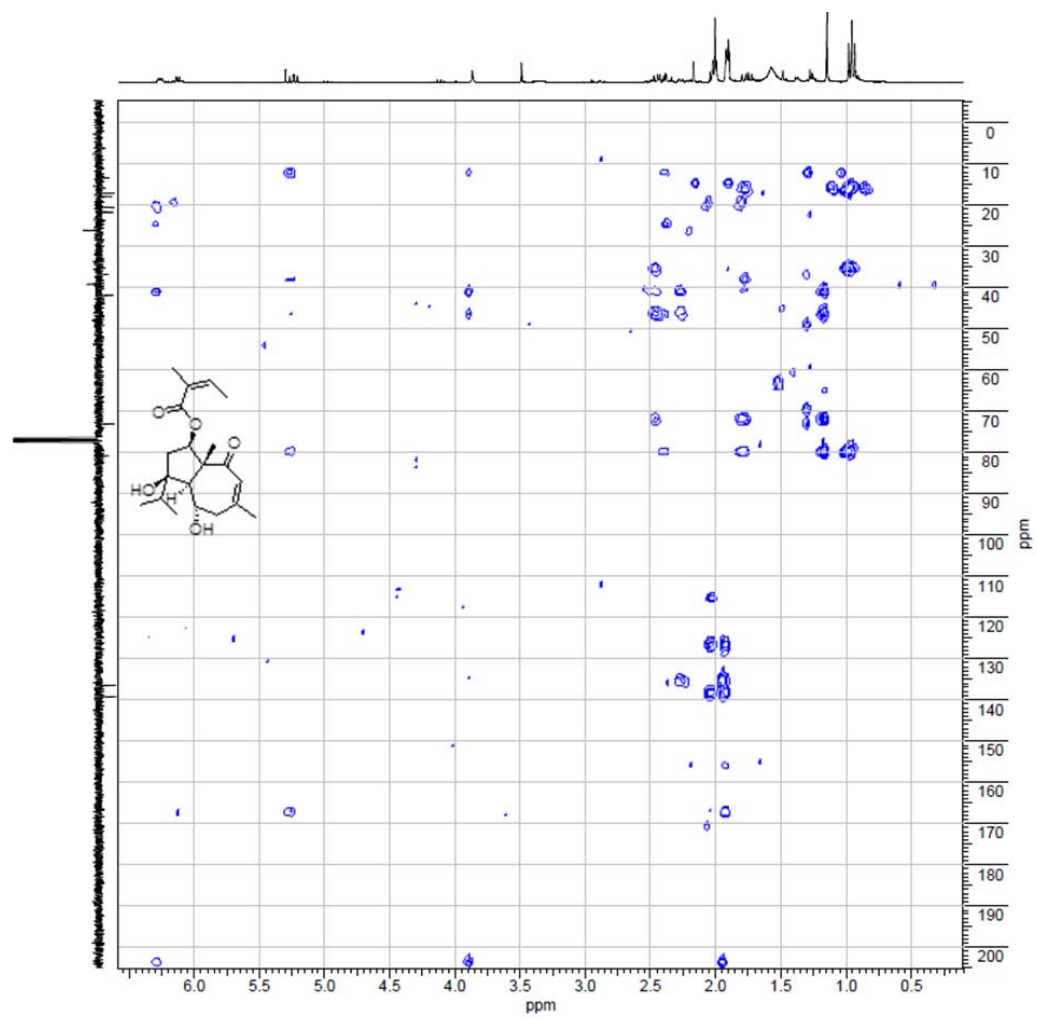
S20. COSY spectrum of compound **3** in CDCl<sub>3</sub>.



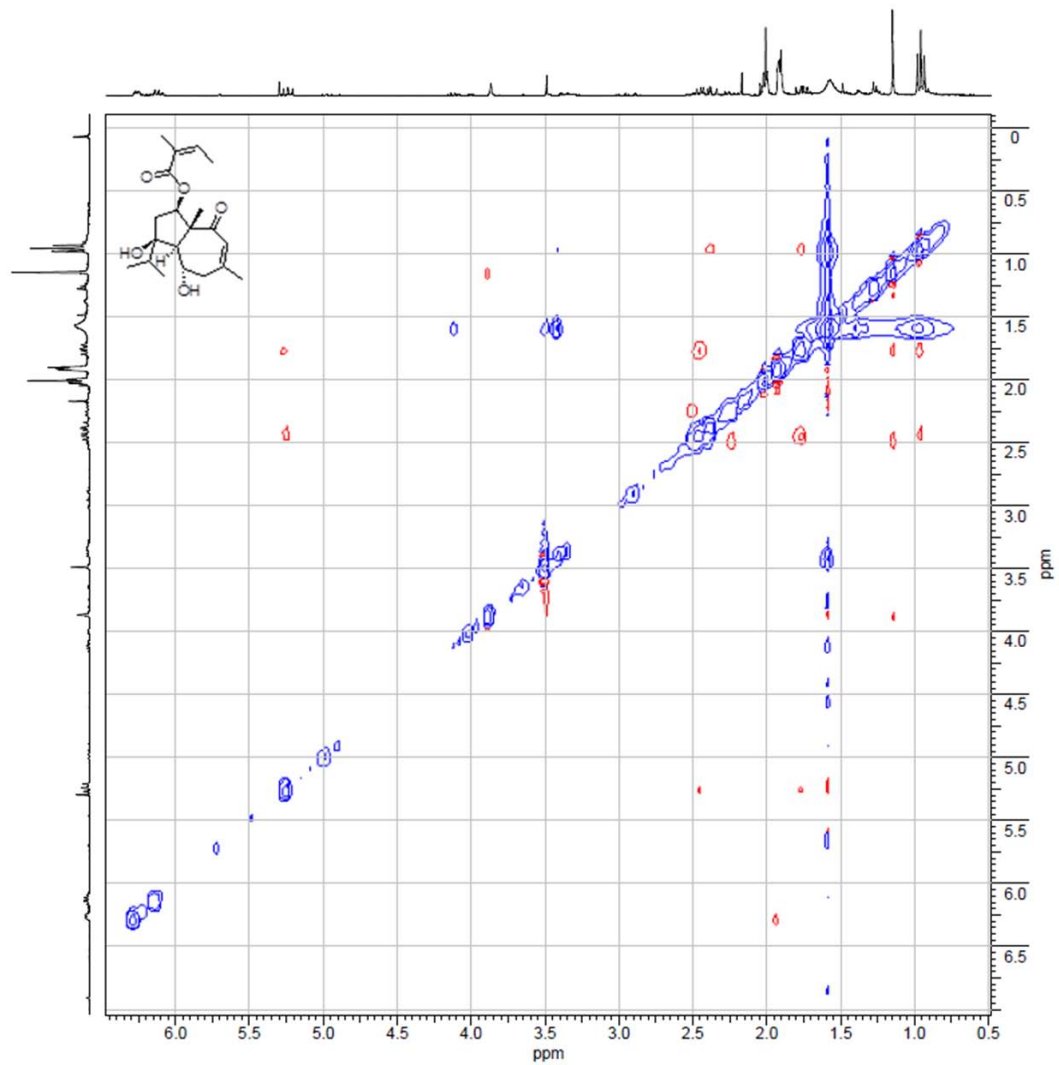
S21. HSQC spectrum of compound **3** in CDCl<sub>3</sub>.



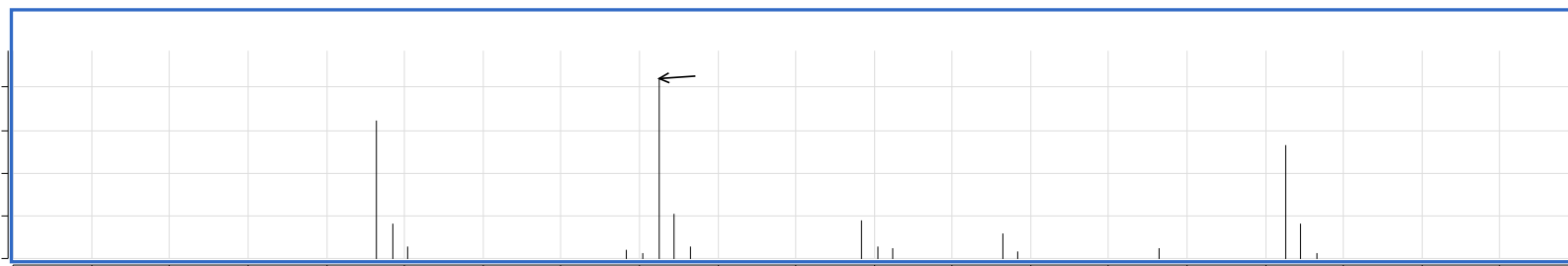
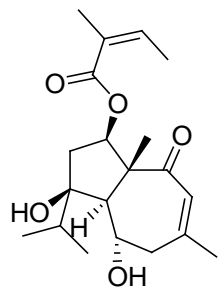
S22. HMBC spectrum of compound **3** in CDCl<sub>3</sub>.



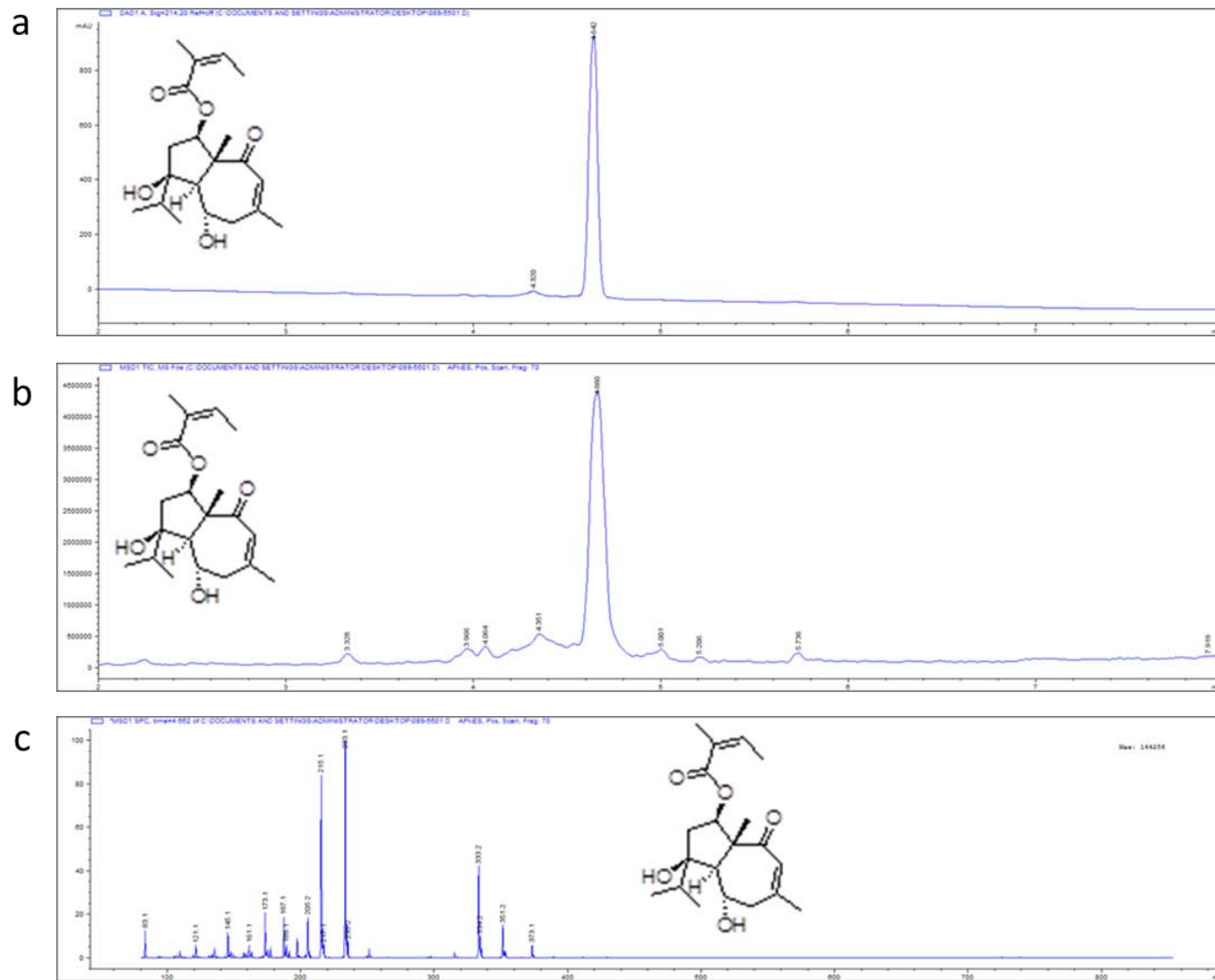
S23. NOESY spectrum of compound **3** in CDCl<sub>3</sub>.



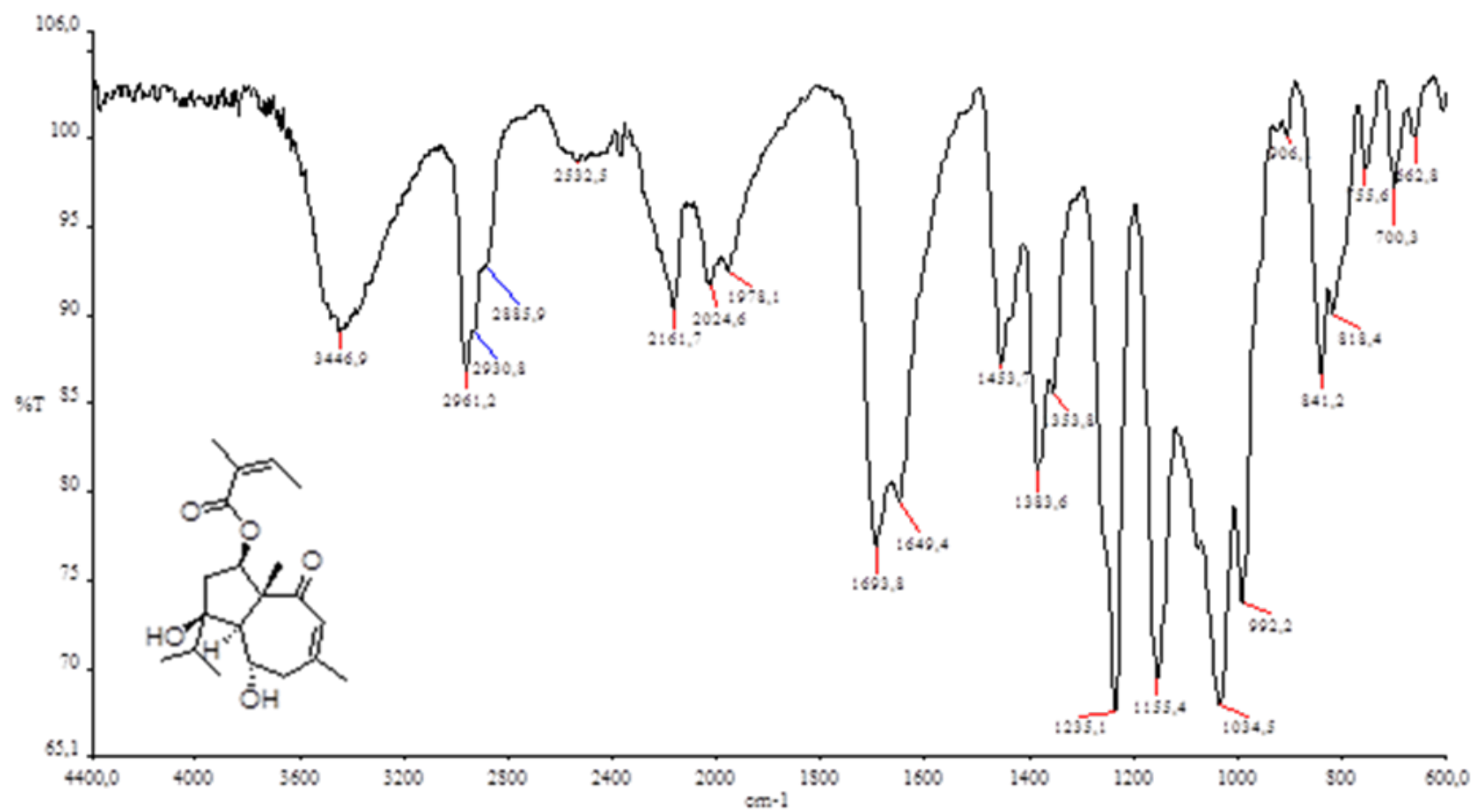
S24. HR-MS spectrum of compound 3.



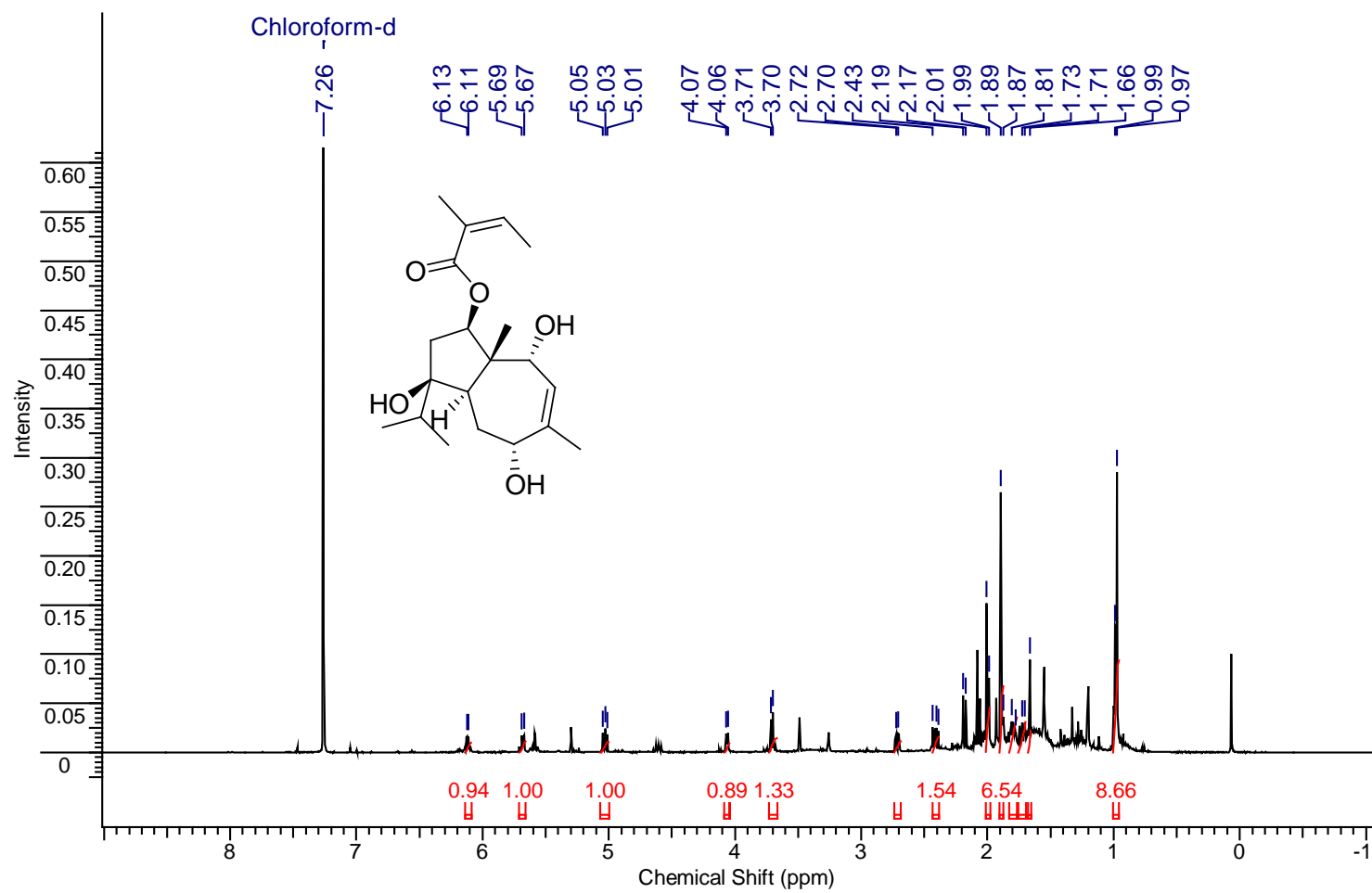
S25. LC-MS data for compound **3**. a) LC-MS chromatogram; b) Total Ion Current chromatogram; c) fragmentation spectrum of the peak of compound **3**.



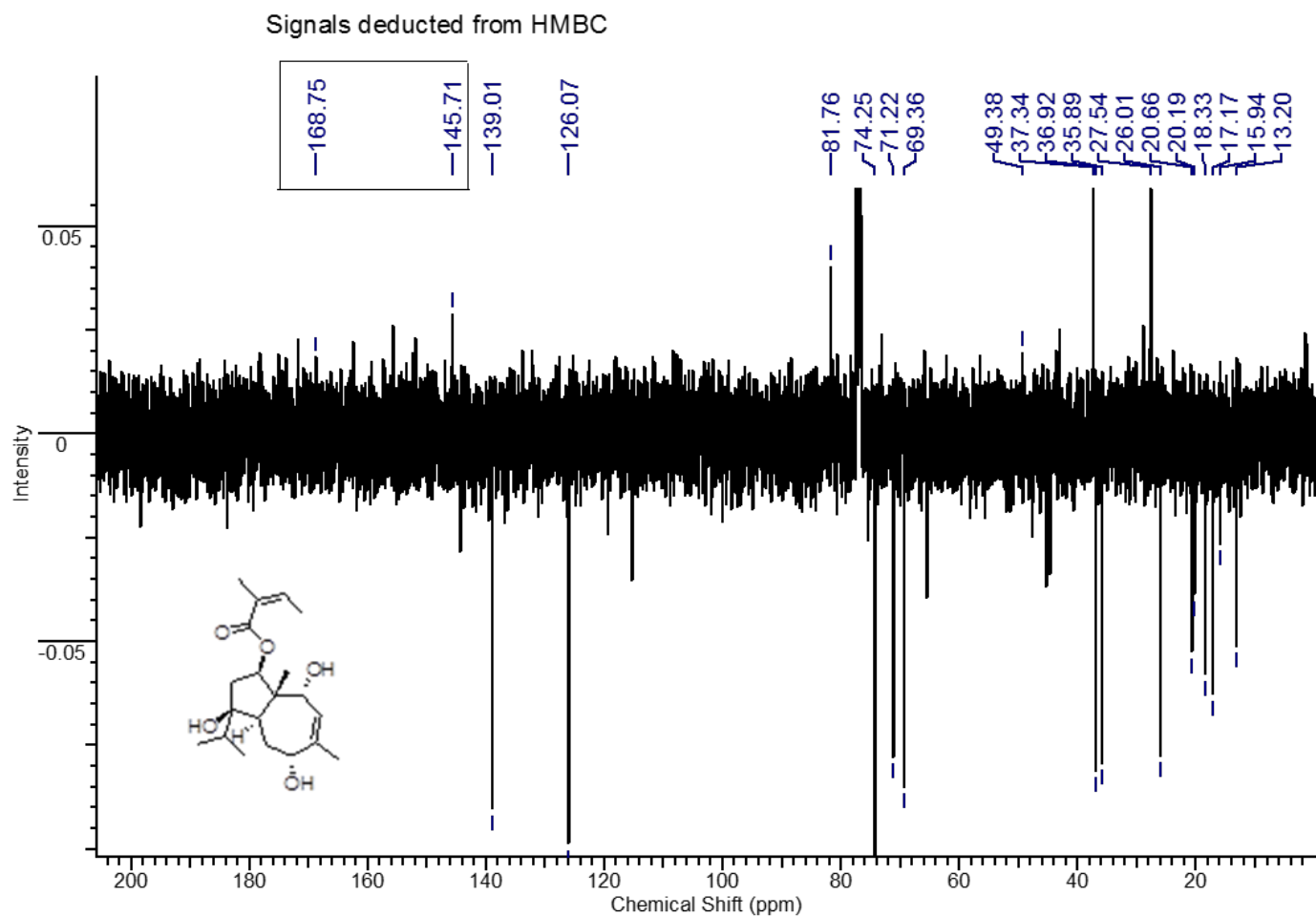
S26. IR spectrum of compound 3.



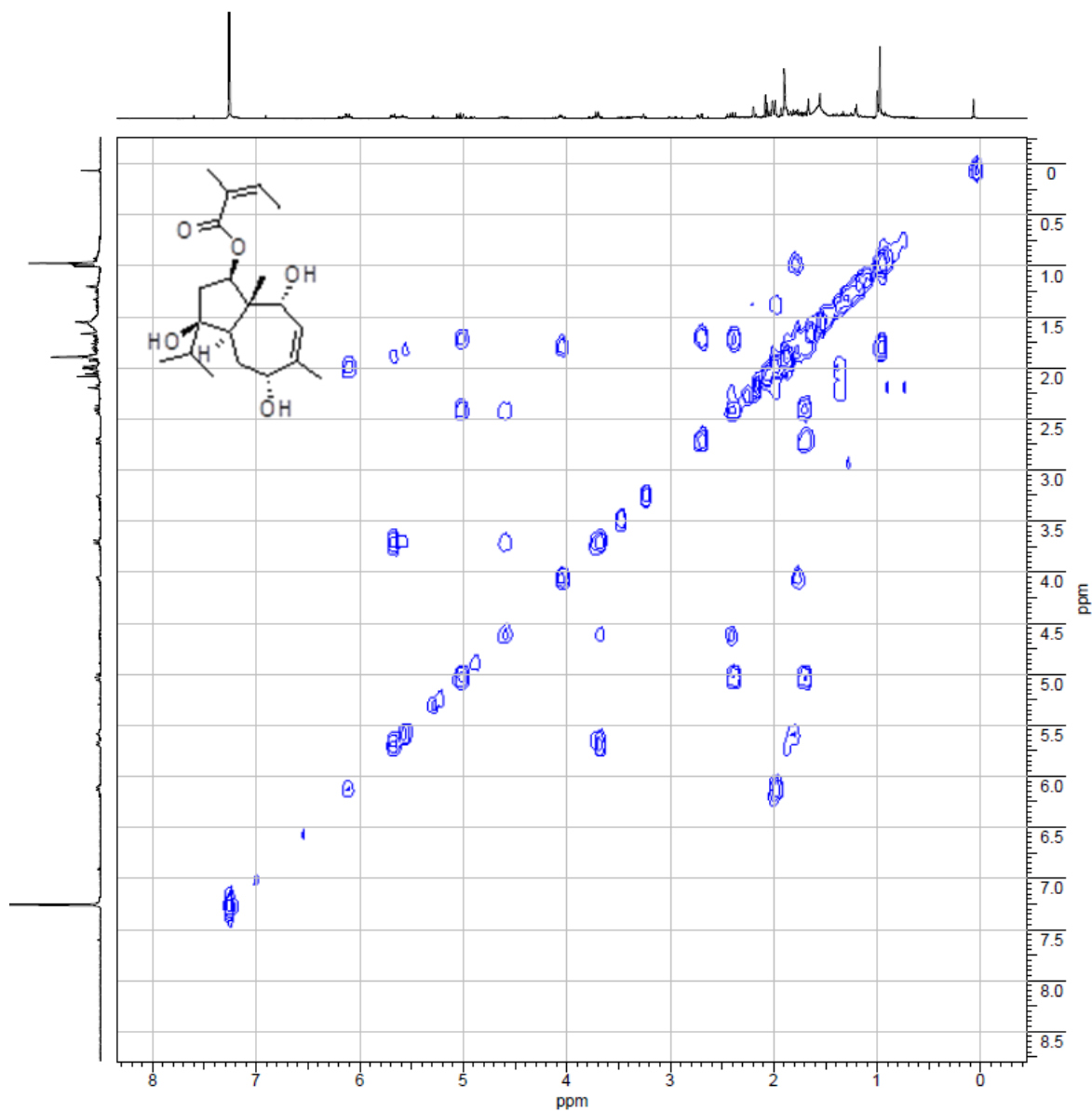
S27. <sup>1</sup>H NMR Spectrum of compound **4** (500 MHz) in CDCl<sub>3</sub>.



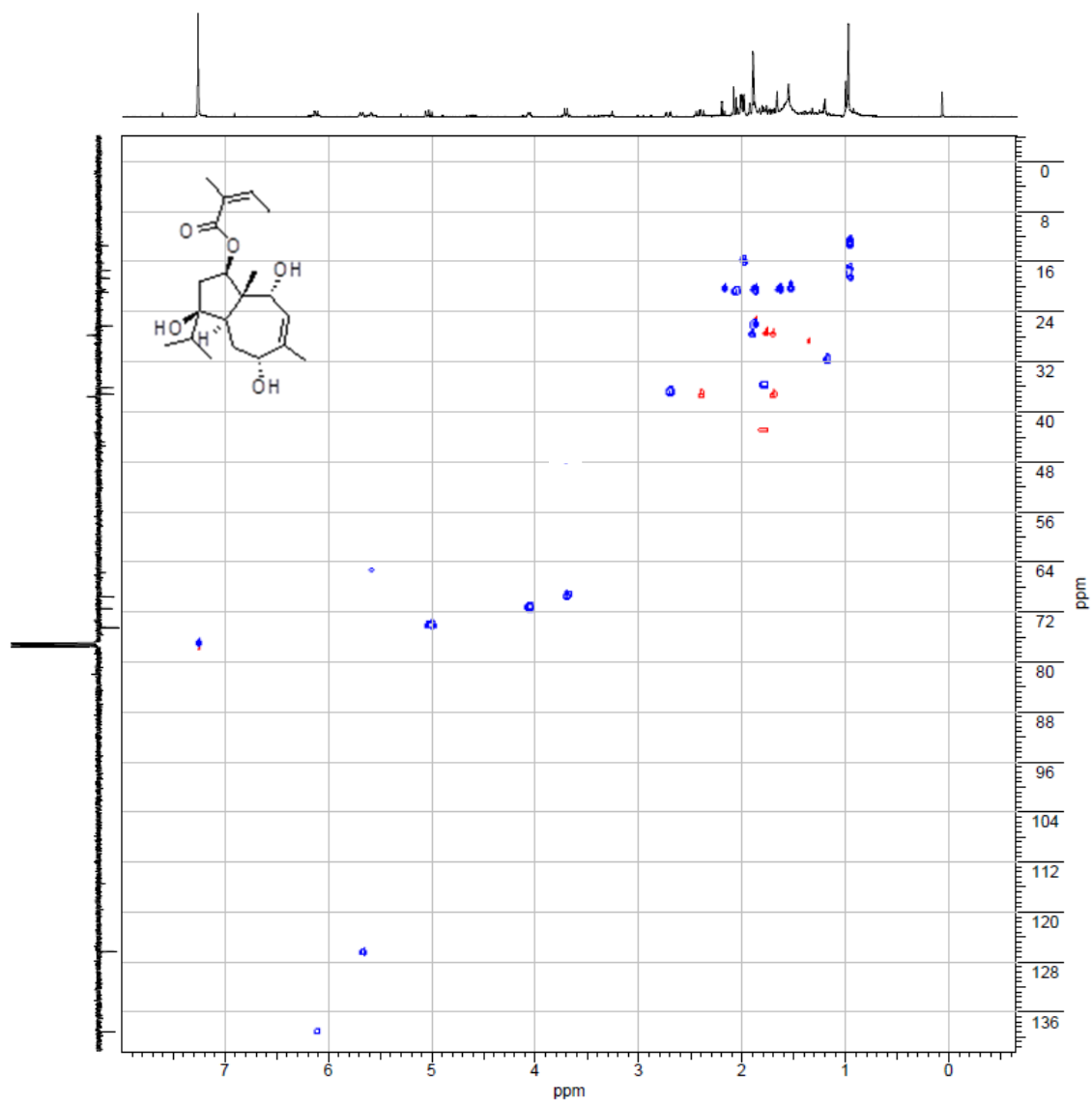
S28. APT spectrum of compound **4** (125 MHz) in CDCl<sub>3</sub>.



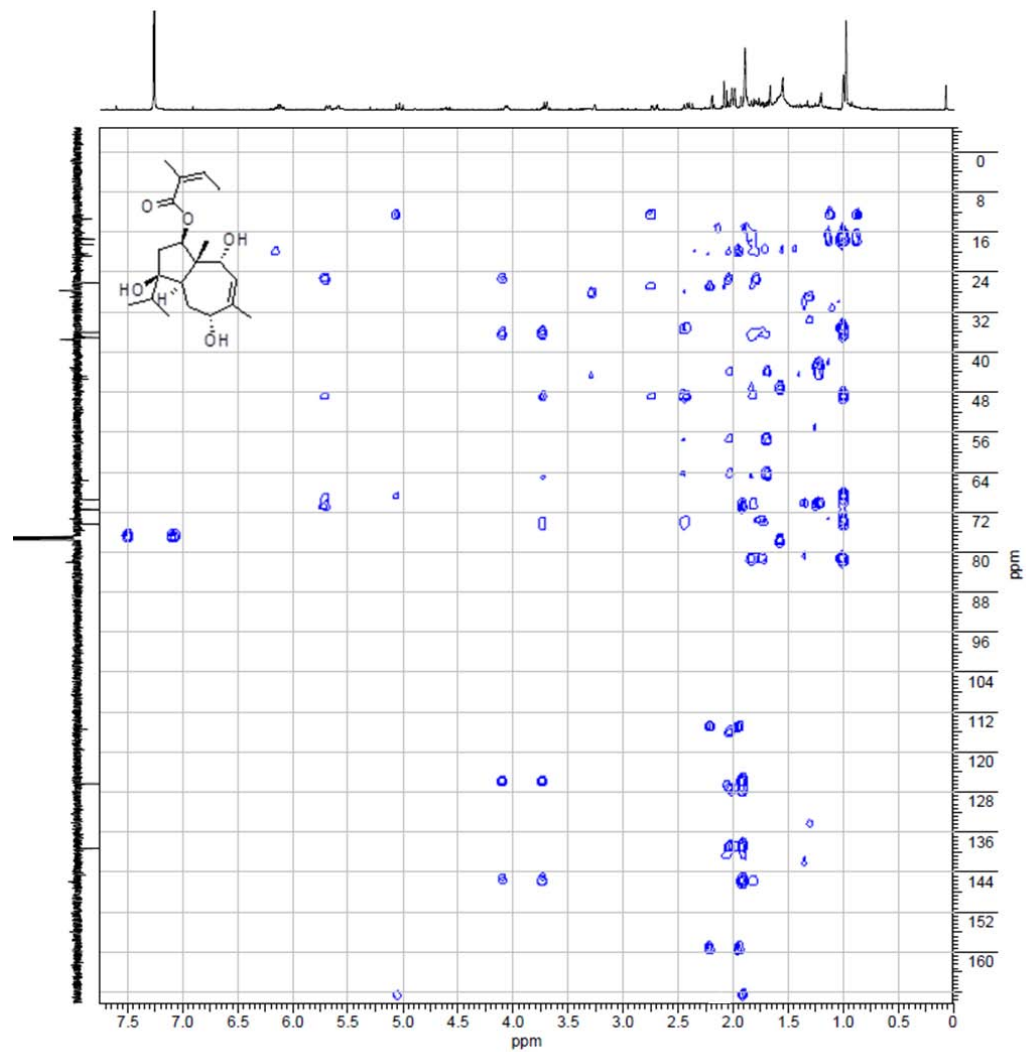
S29. COSY spectrum of compound **4** in CDCl<sub>3</sub>.



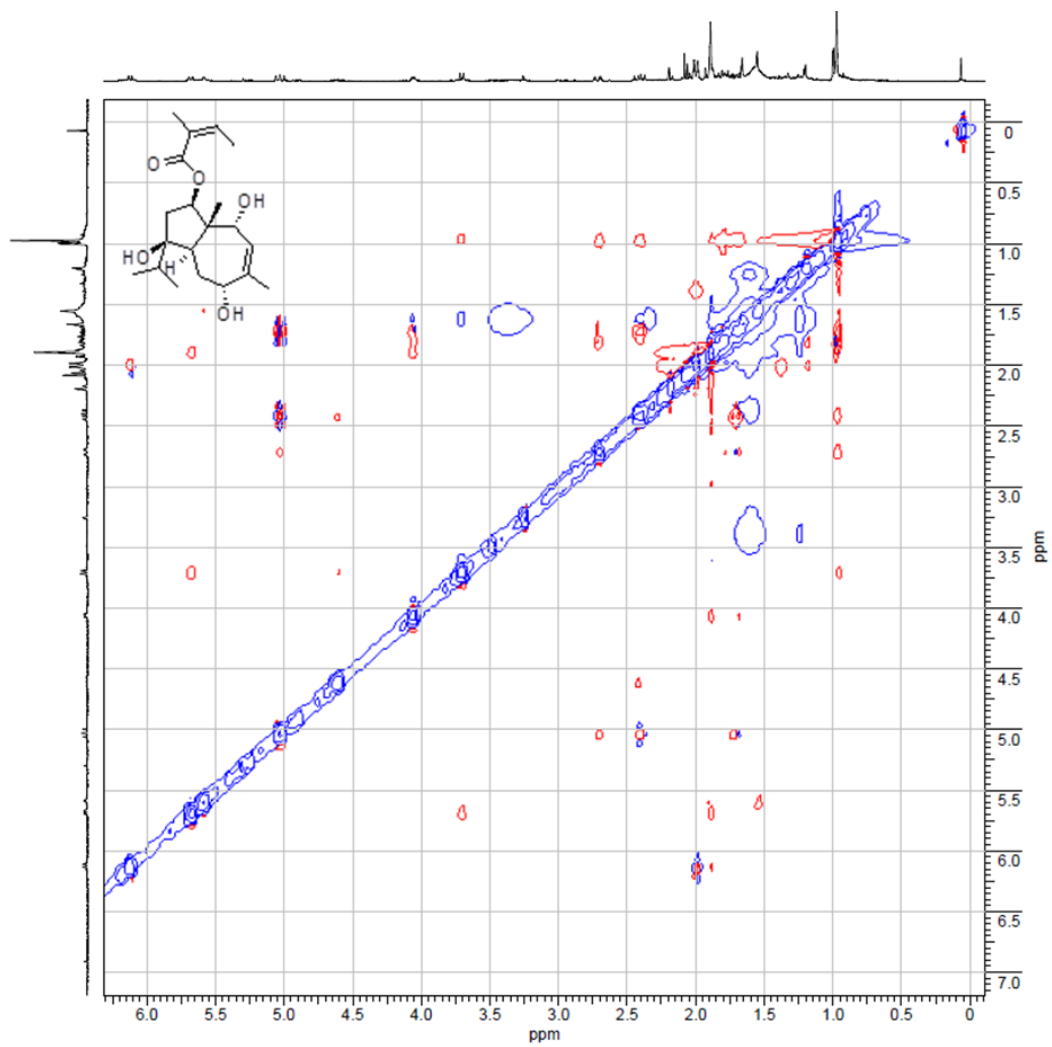
S30. HSQC spectrum of compound **4** in CDCl<sub>3</sub>.



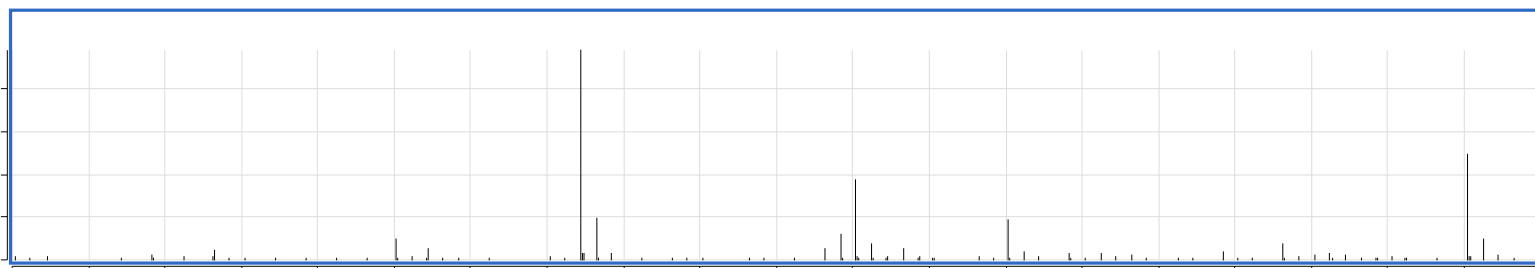
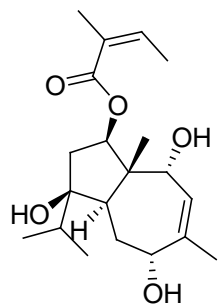
S31. HMBC spectrum of compound **4** in CDCl<sub>3</sub>.



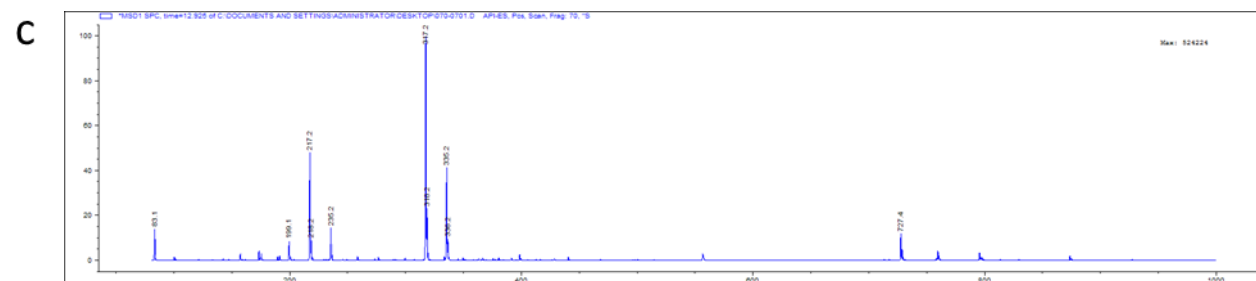
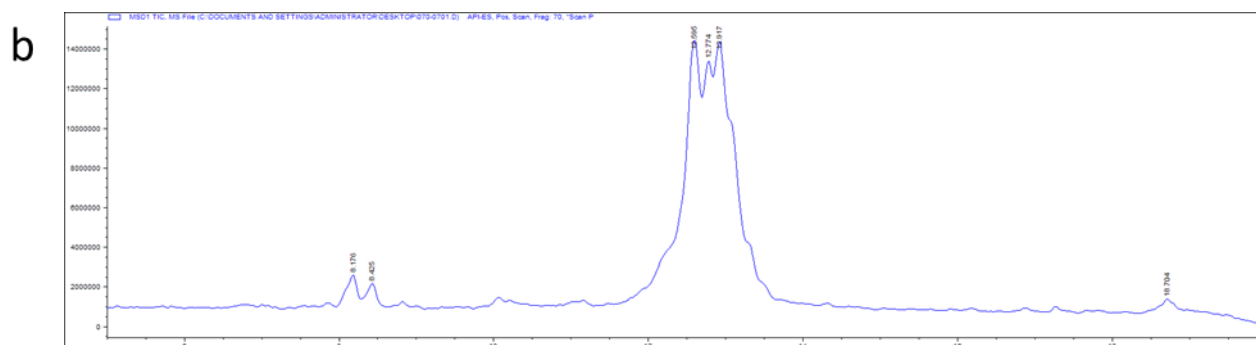
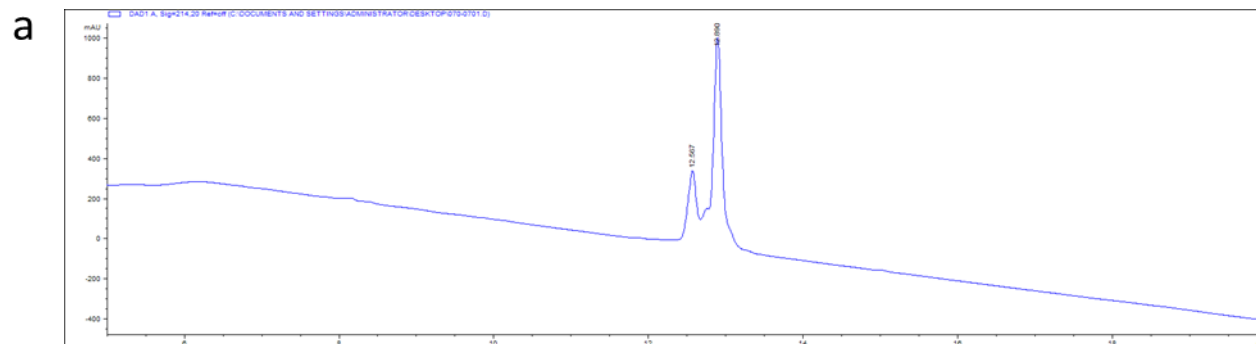
S32. NOESY spectrum of compound **4** in CDCl<sub>3</sub>.



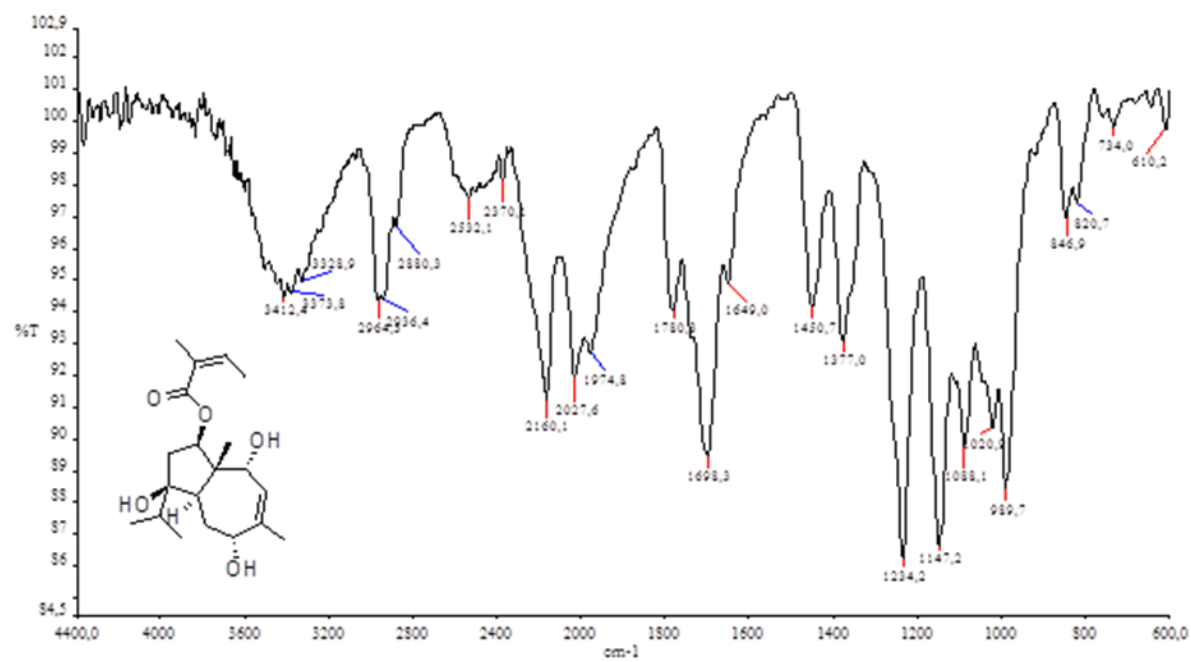
S33. HR-MS spectrum of compound 4.



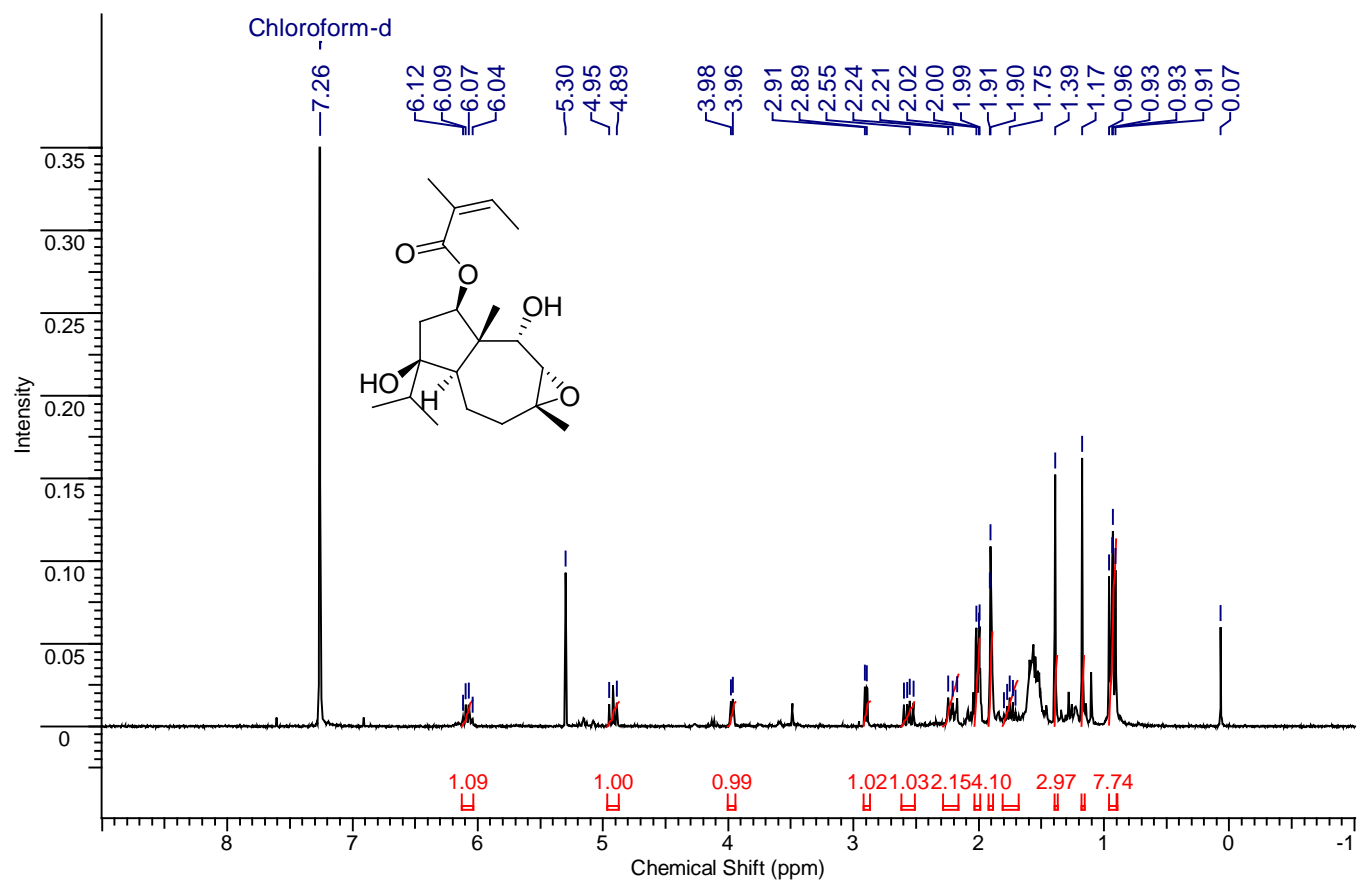
S34. LC-MS data for compound **4**. a) LC-MS chromatogram; b) Total Ion Current chromatogram; c) fragmentation spectrum of the peak of compound **4**.



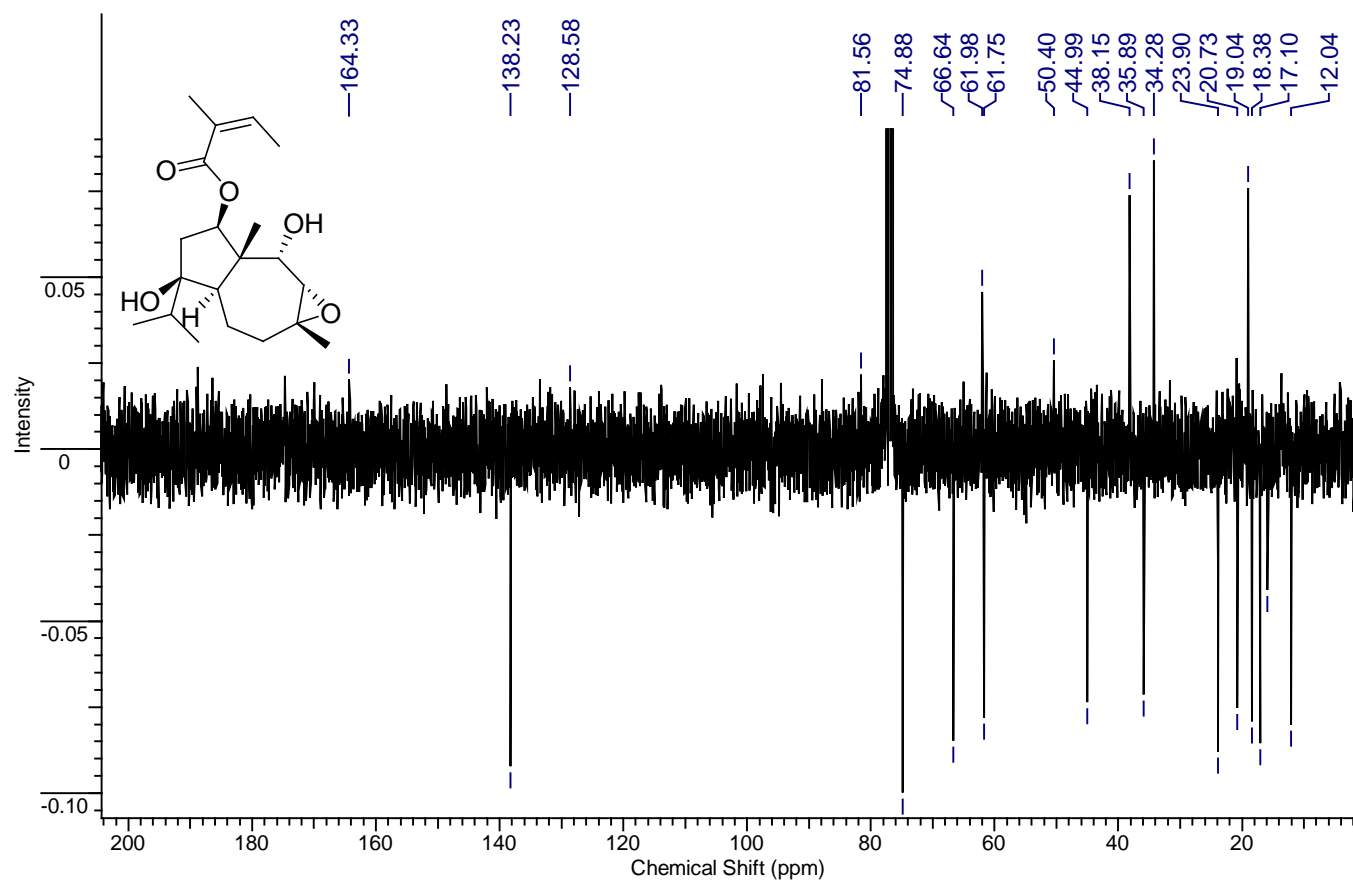
S35. IR spectrum of compound 4.



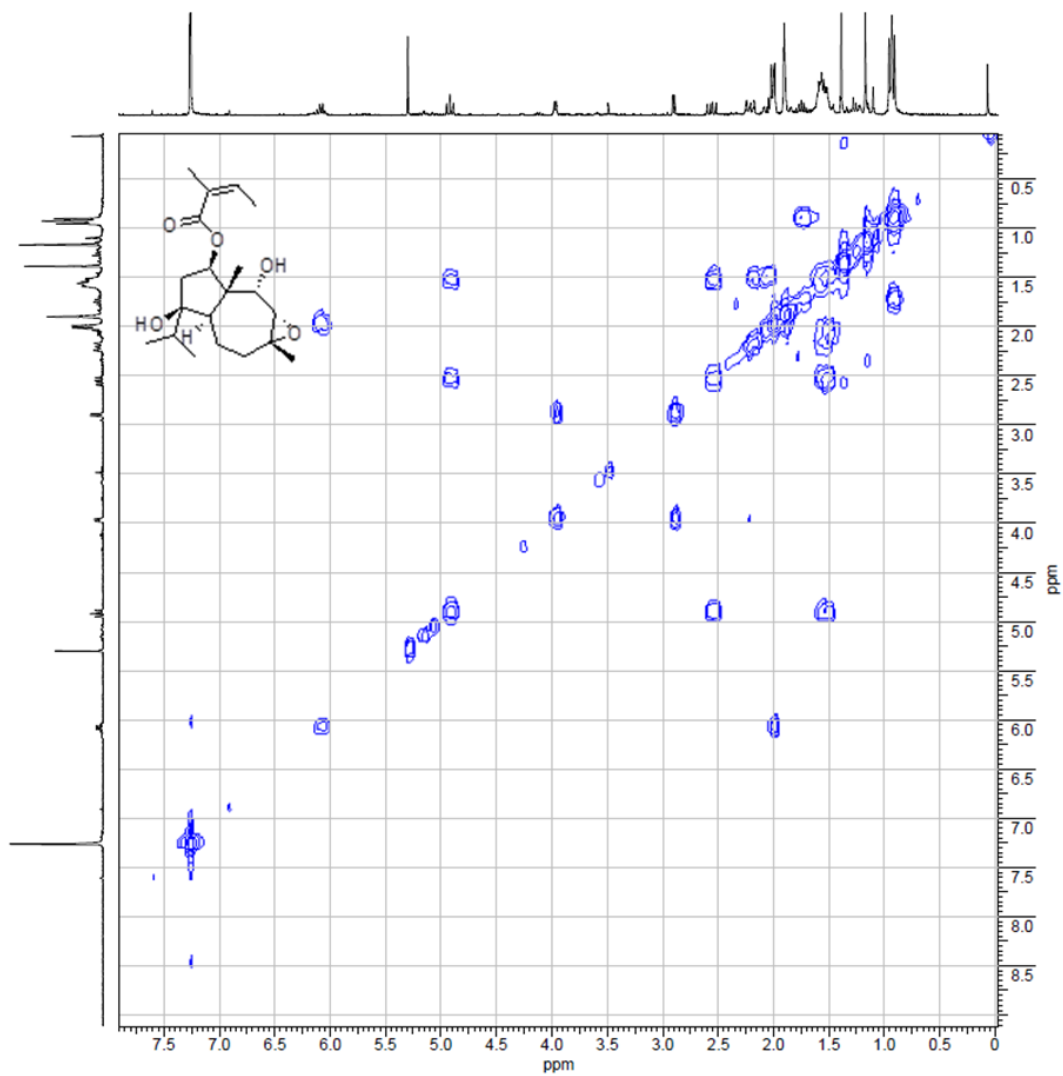
S36.  $^1\text{H}$  NMR Spectrum of compound **5** (300 MHz) in  $\text{CDCl}_3$ .



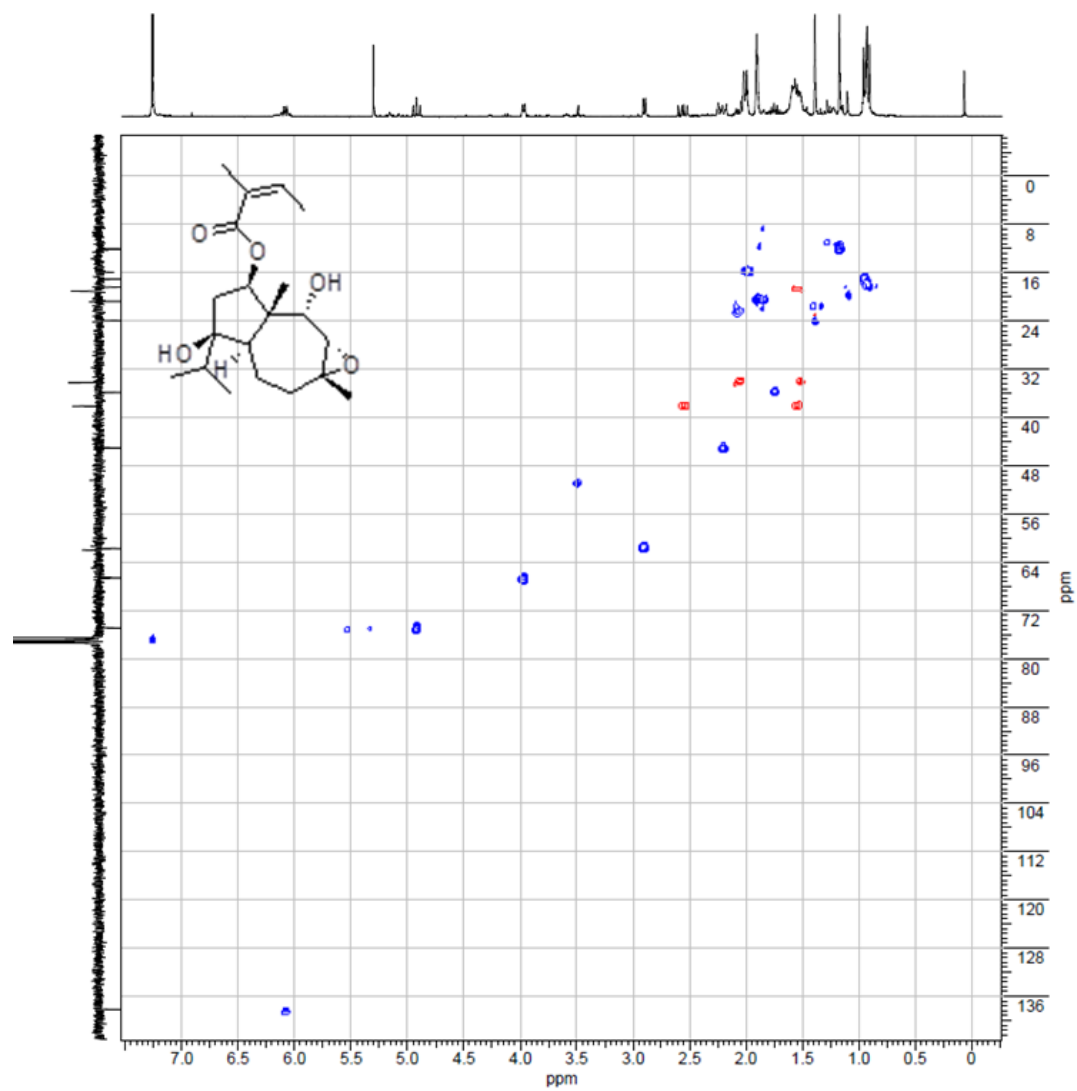
S37. APT spectrum of compound **5** (75 MHz) in CDCl<sub>3</sub>.



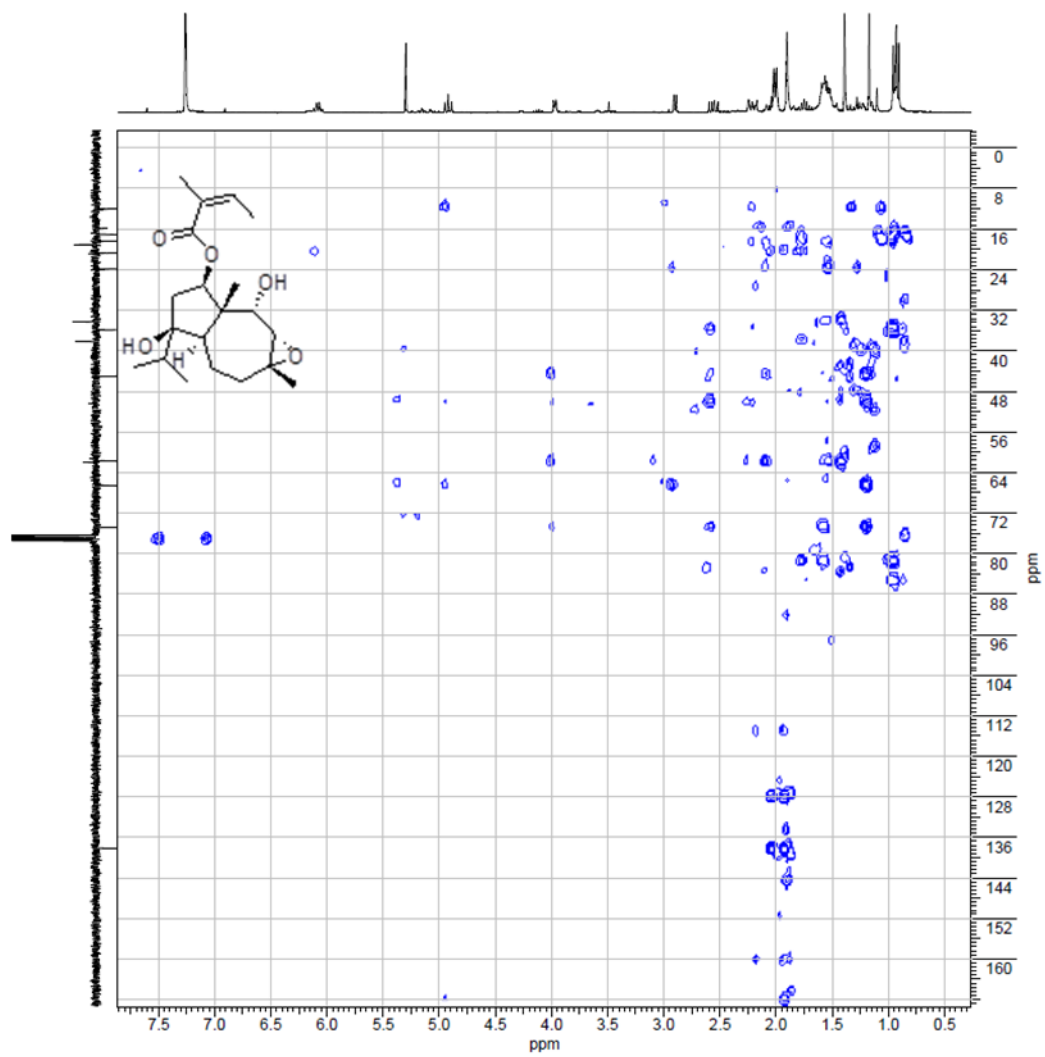
S38. COSY spectrum of compound **5** in CDCl<sub>3</sub>.



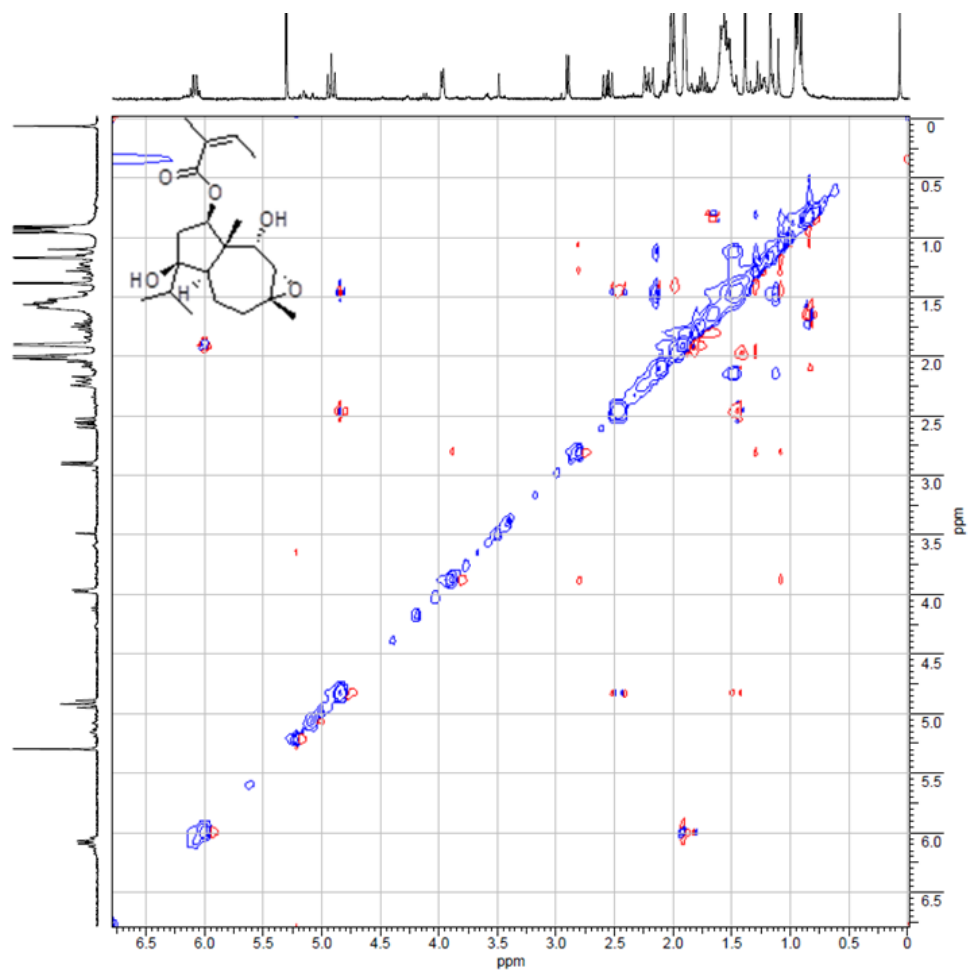
S38. HSQC spectrum of compound **5** in CDCl<sub>3</sub>.



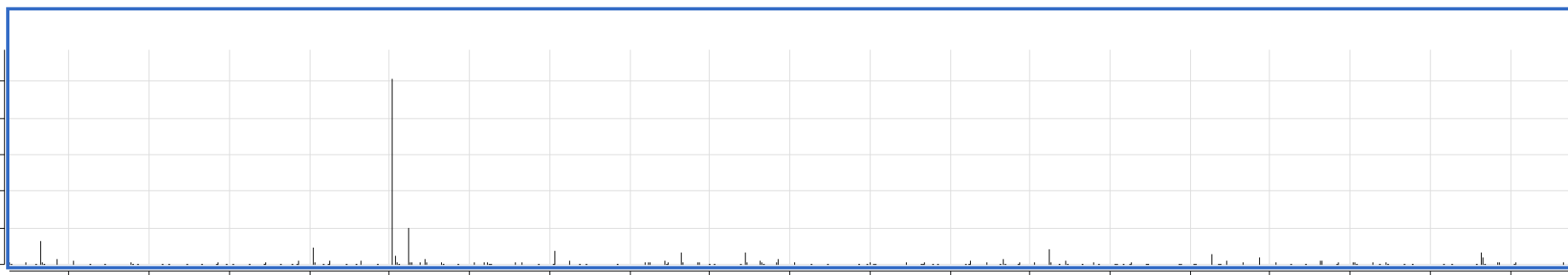
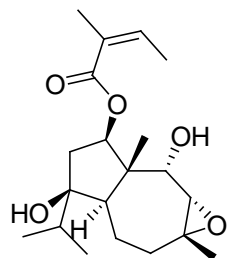
S40. HMBC spectrum of compound **5** in CDCl<sub>3</sub>.



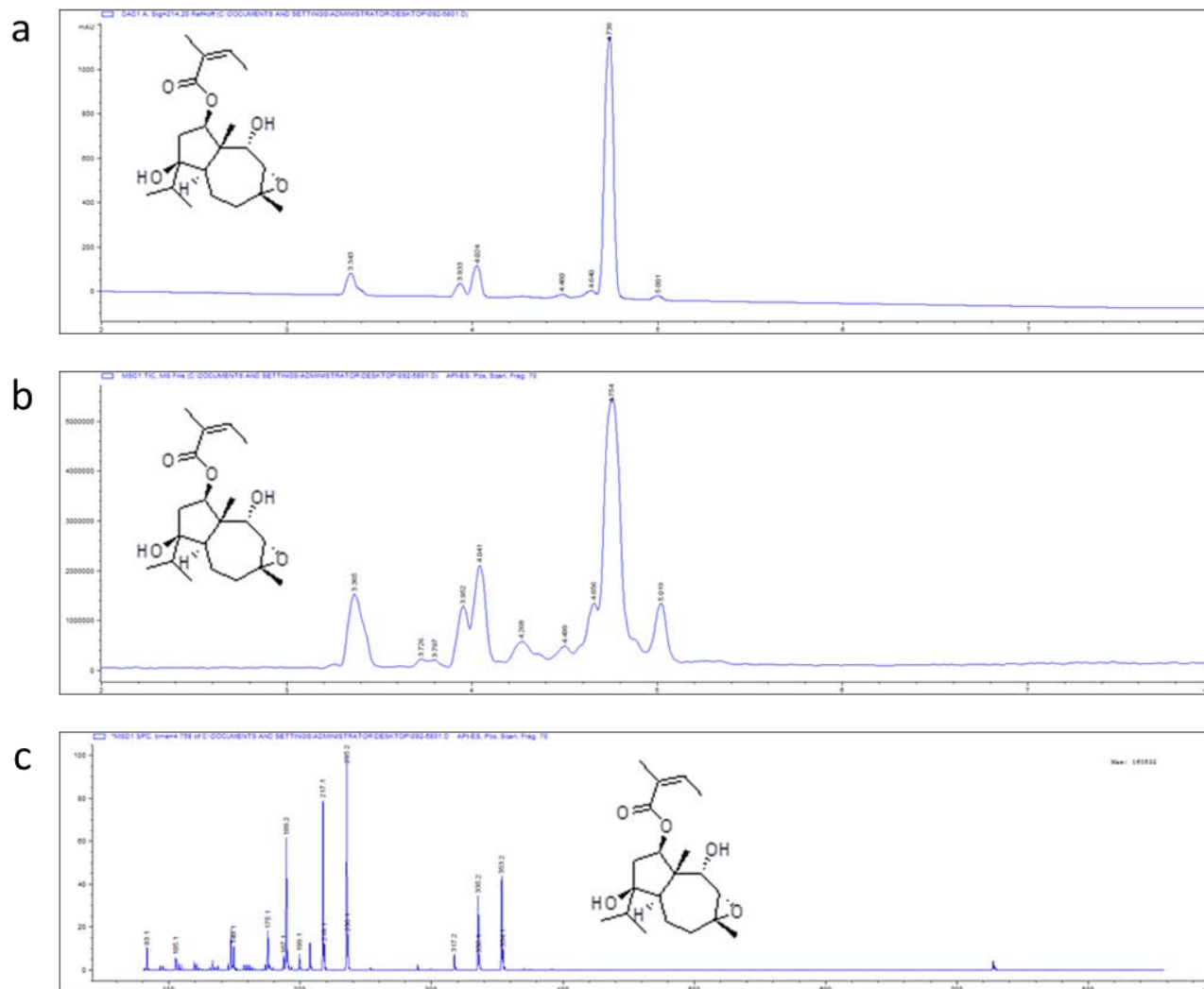
S41. NOESY spectrum of compound **5** in CDCl<sub>3</sub>.



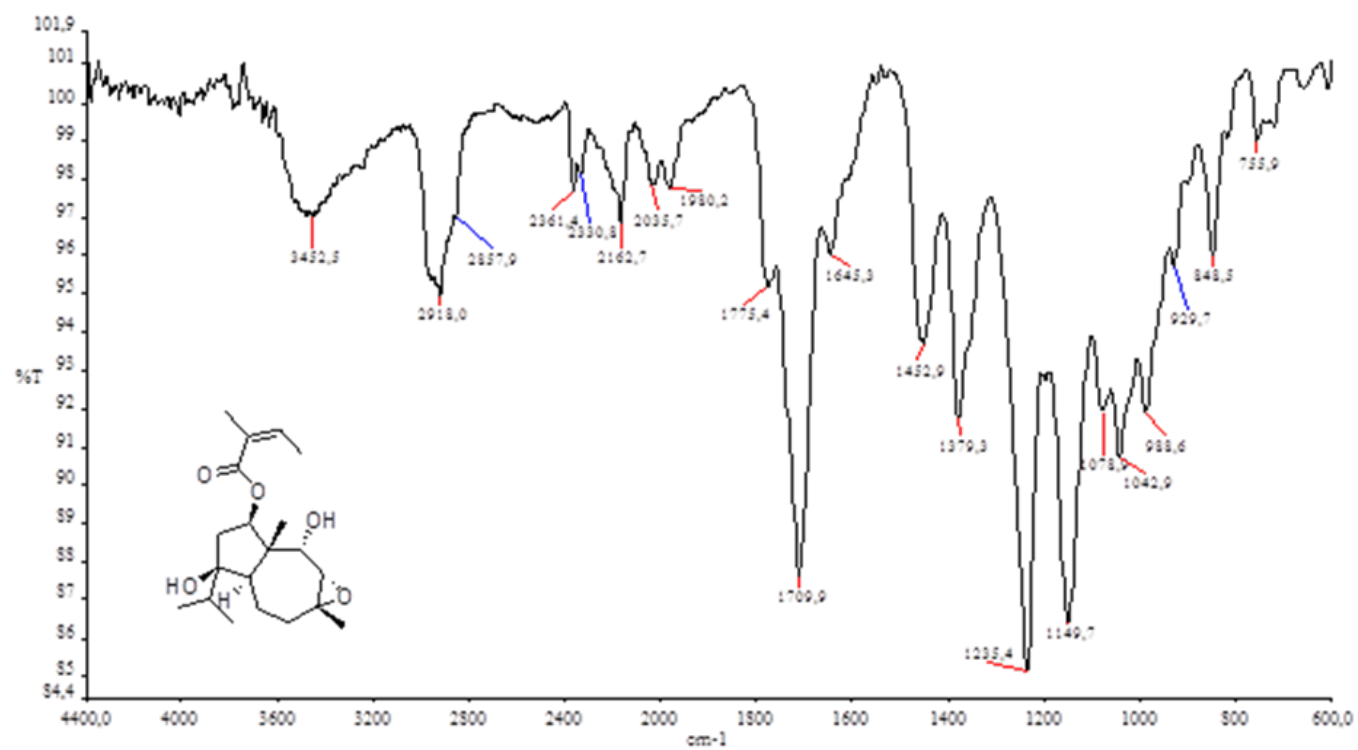
S42. HR-MS spectrum of compound **5**.



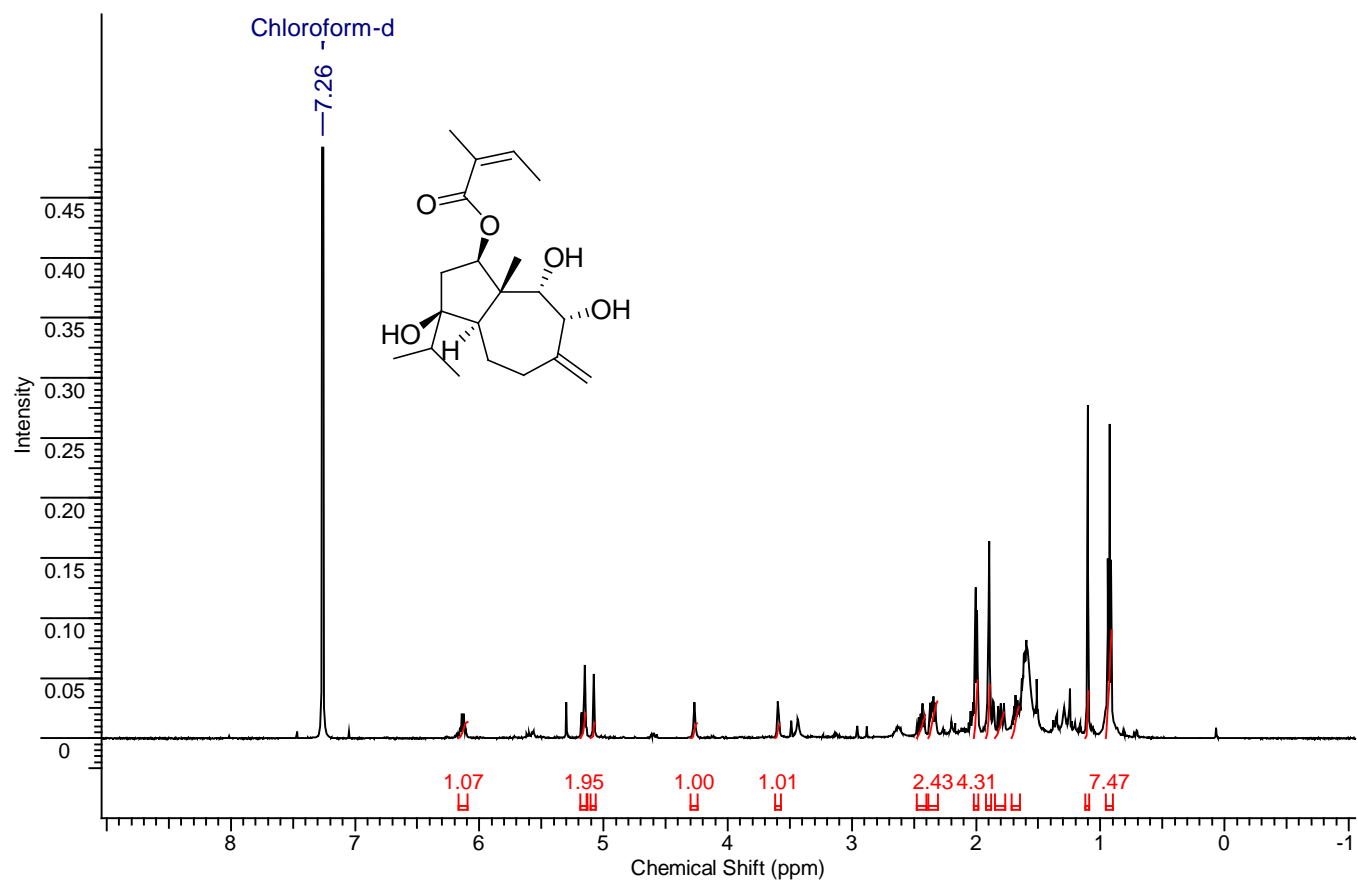
S43. LC-MS data for compound **5**. a) LC-MS chromatogram; b) Total Ion Current chromatogram; c) fragmentation spectrum of the peak of compound **5**.



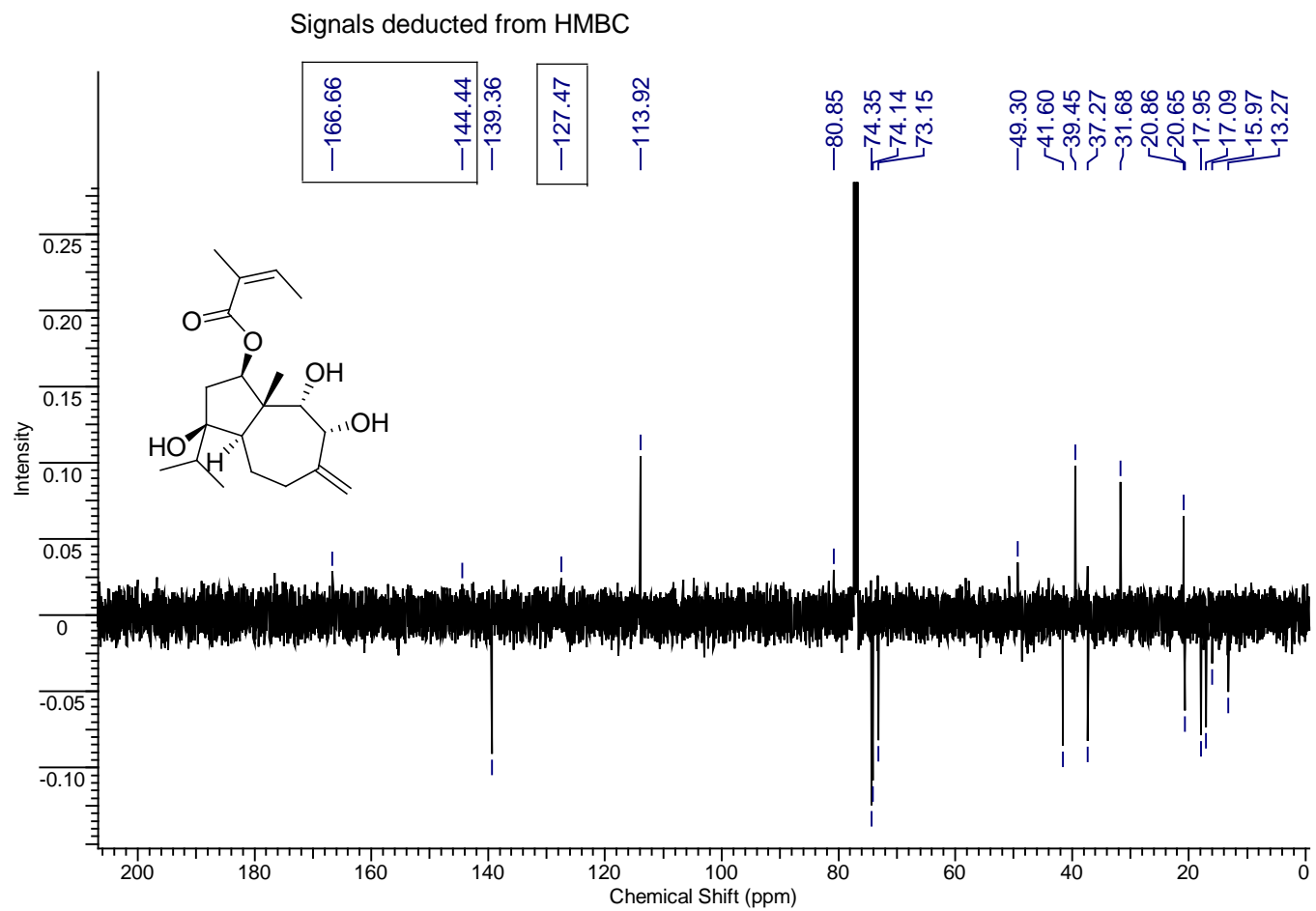
S44. IR spectrum of compound 5.



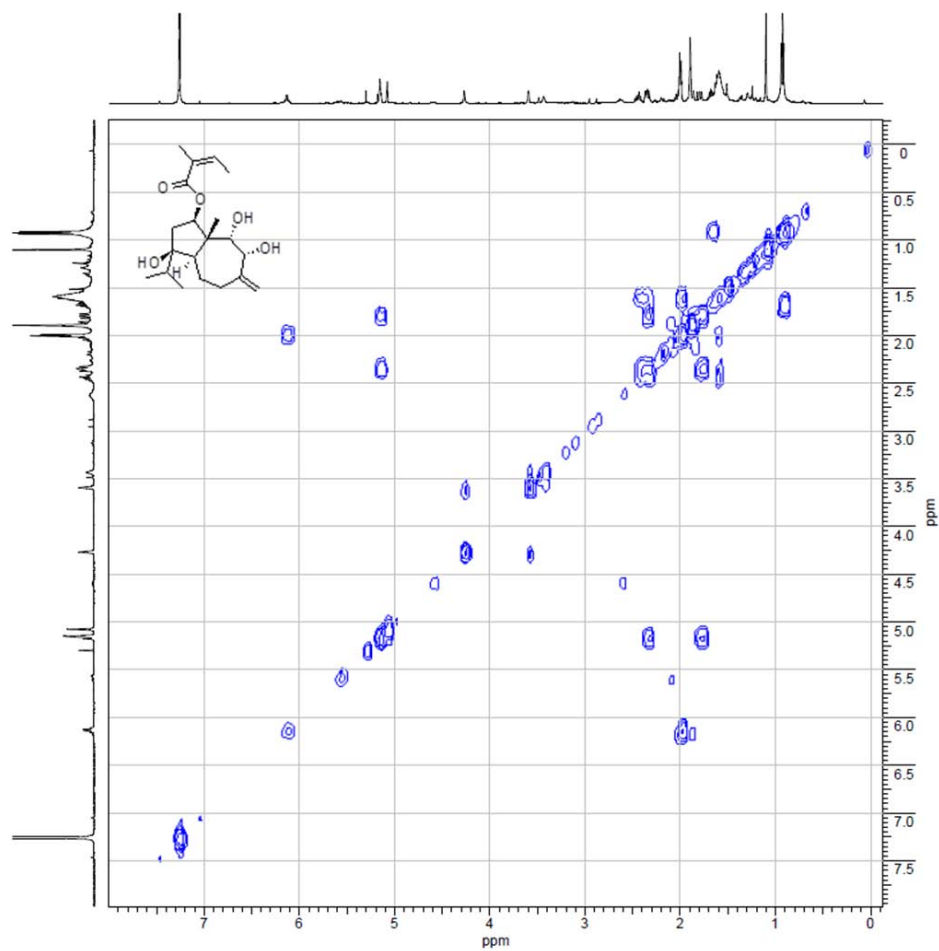
S45.  $^1\text{H}$  NMR Spectrum of compound **6** (500 MHz) in  $\text{CDCl}_3$ .



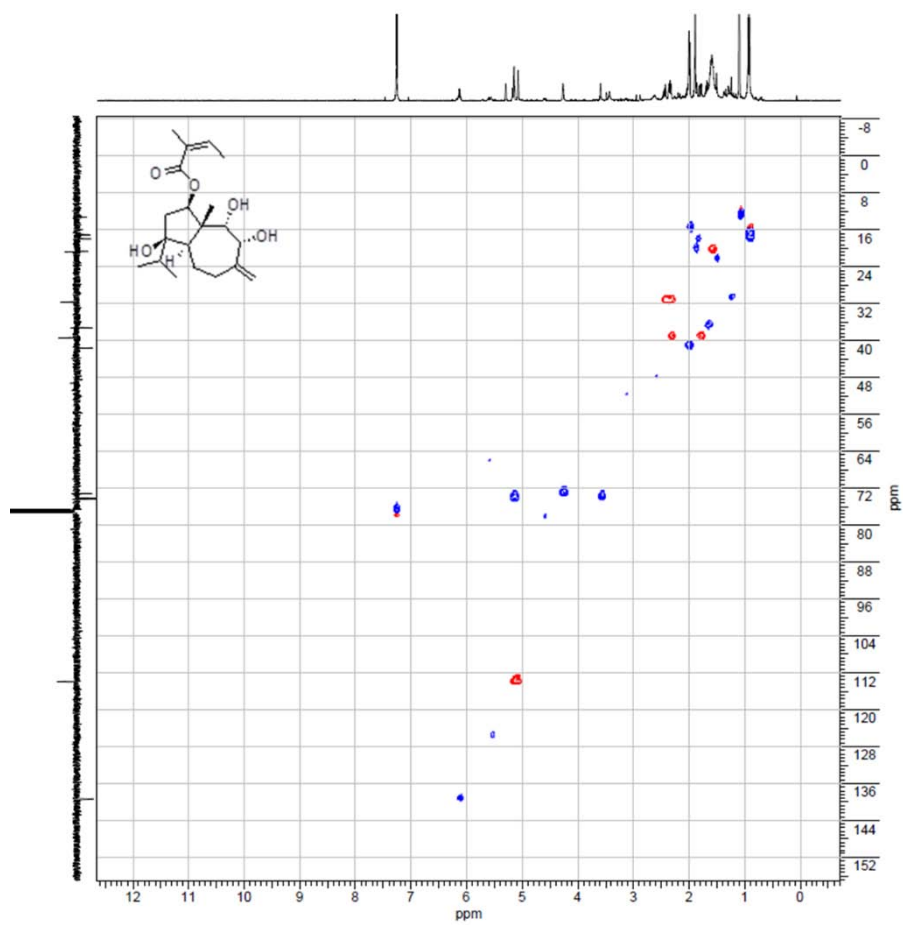
S46. APT spectrum of compound **6** (125 MHz) in CDCl<sub>3</sub>.



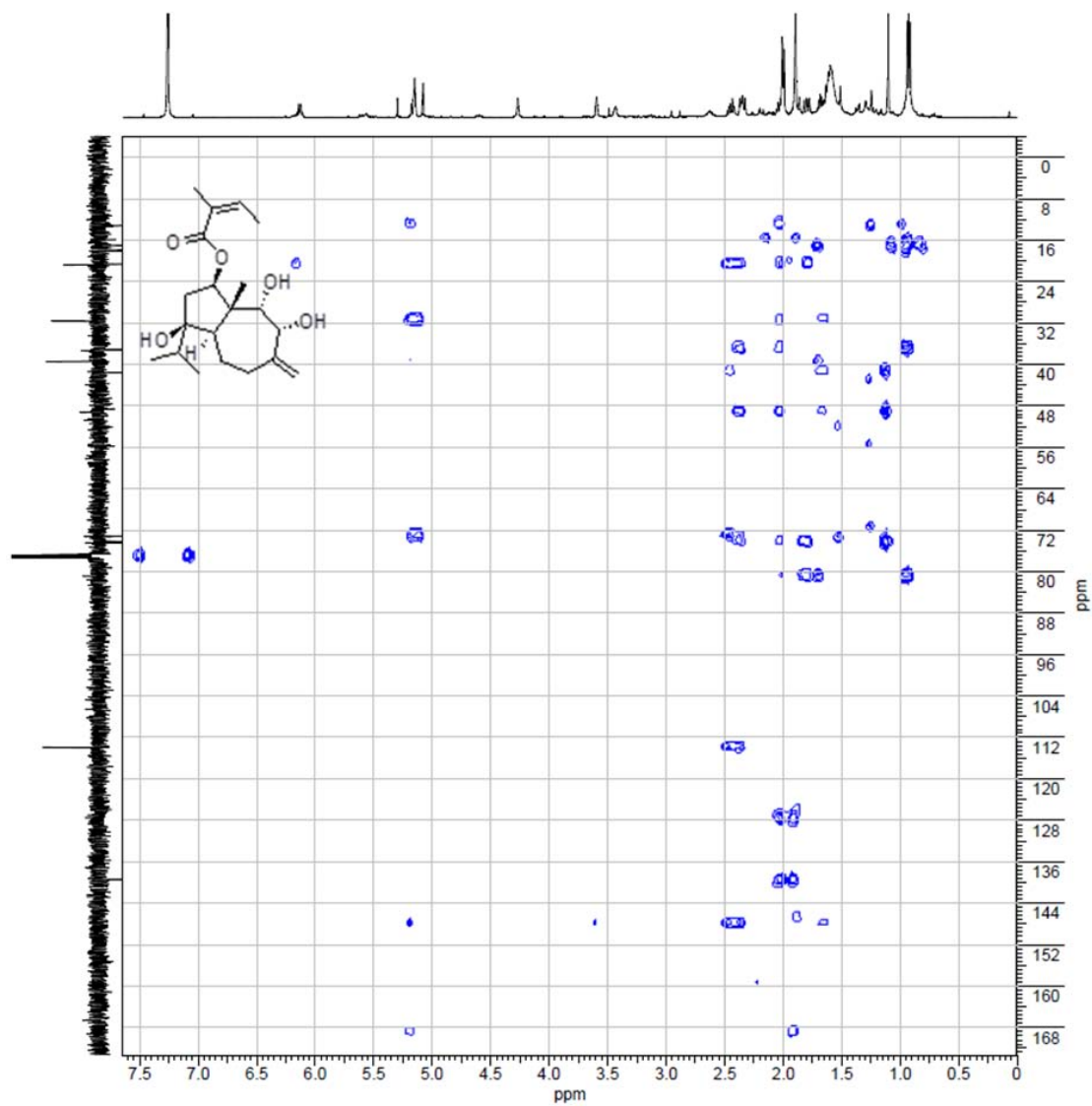
S47. COSY spectrum of compound **6** in CDCl<sub>3</sub>.



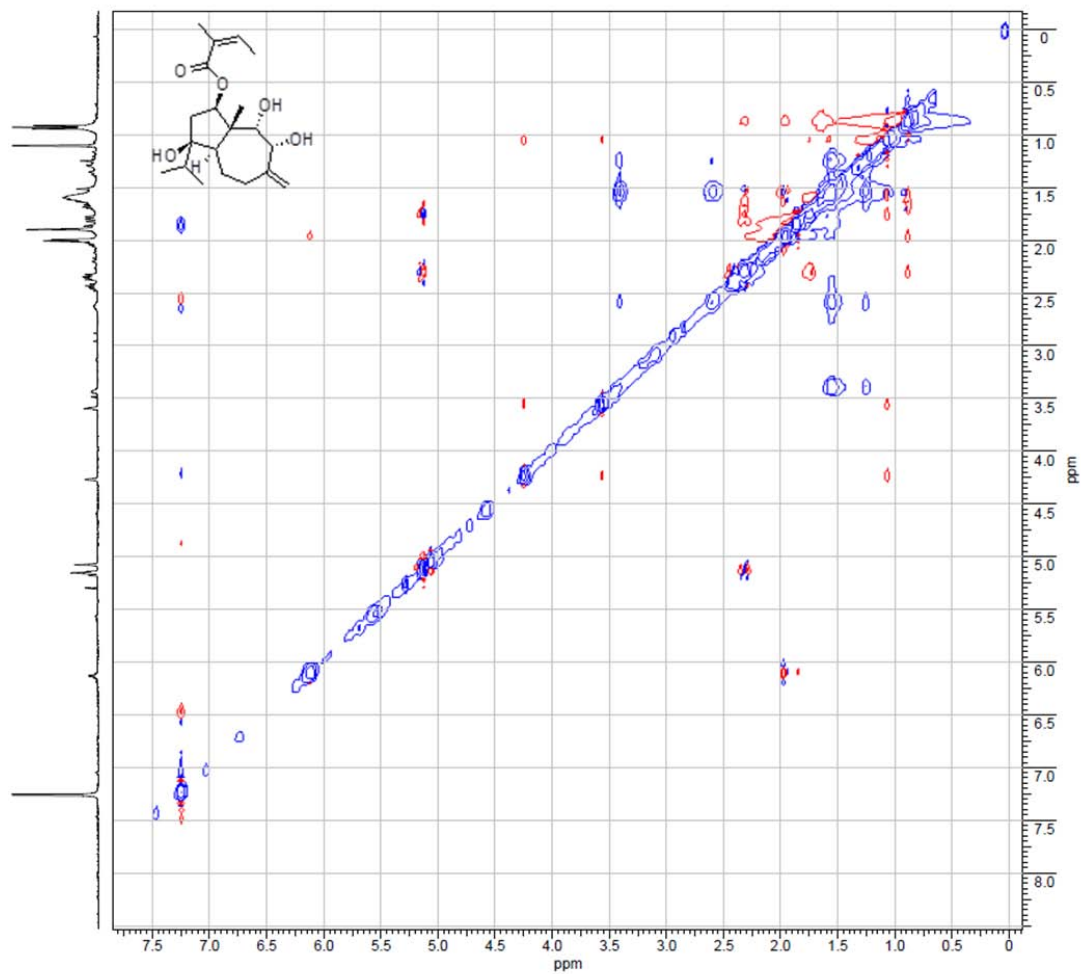
S48. HSQC spectrum of compound **6** in CDCl<sub>3</sub>.



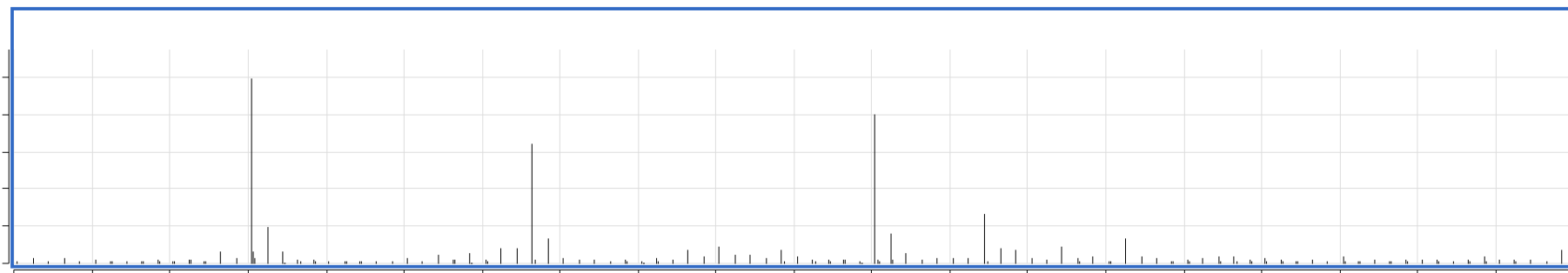
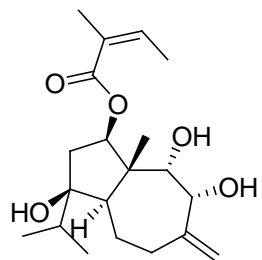
S49. HMBC spectrum of compound **6** in CDCl<sub>3</sub>.



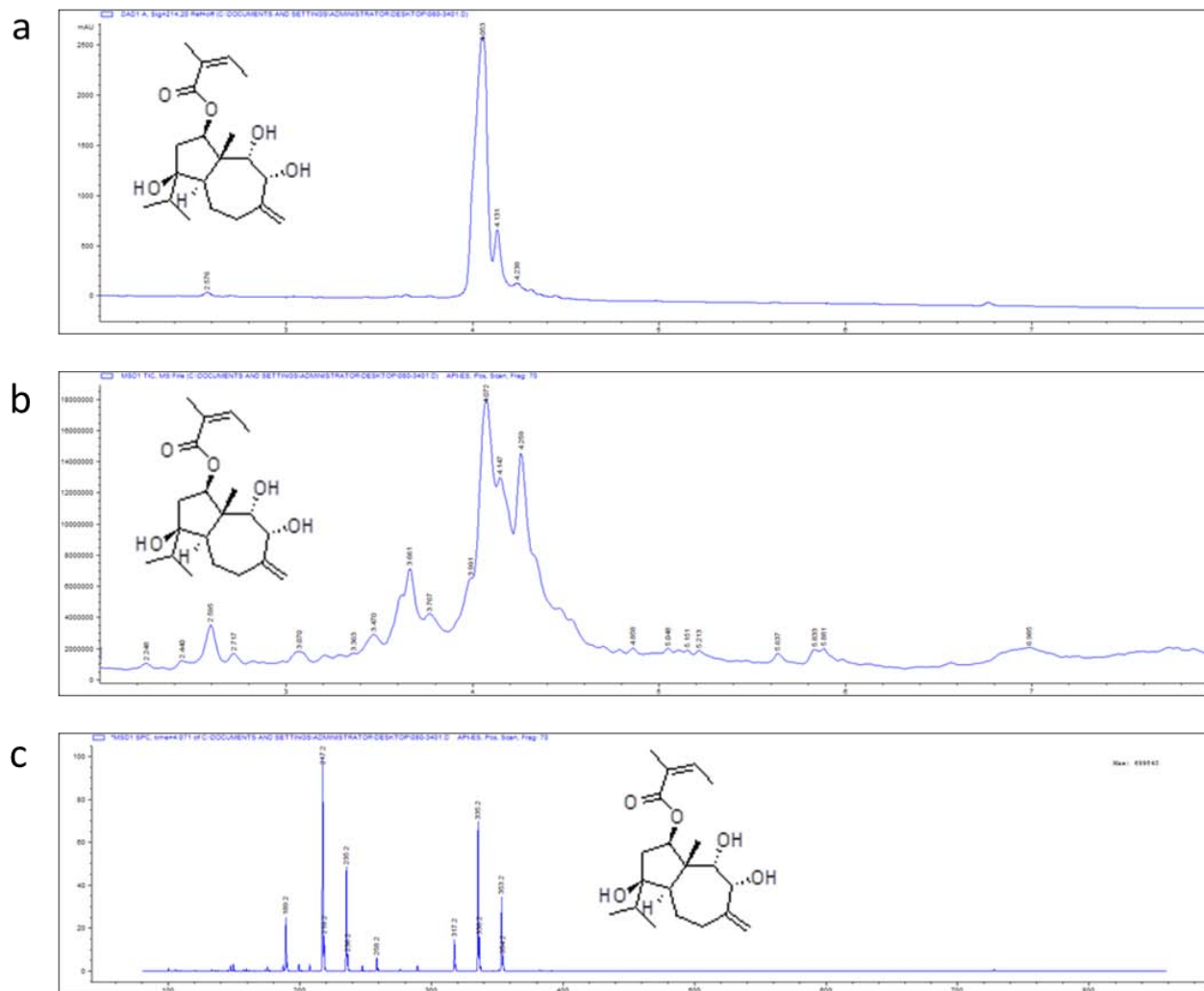
S50. NOESY spectrum of compound **6** in CDCl<sub>3</sub>.



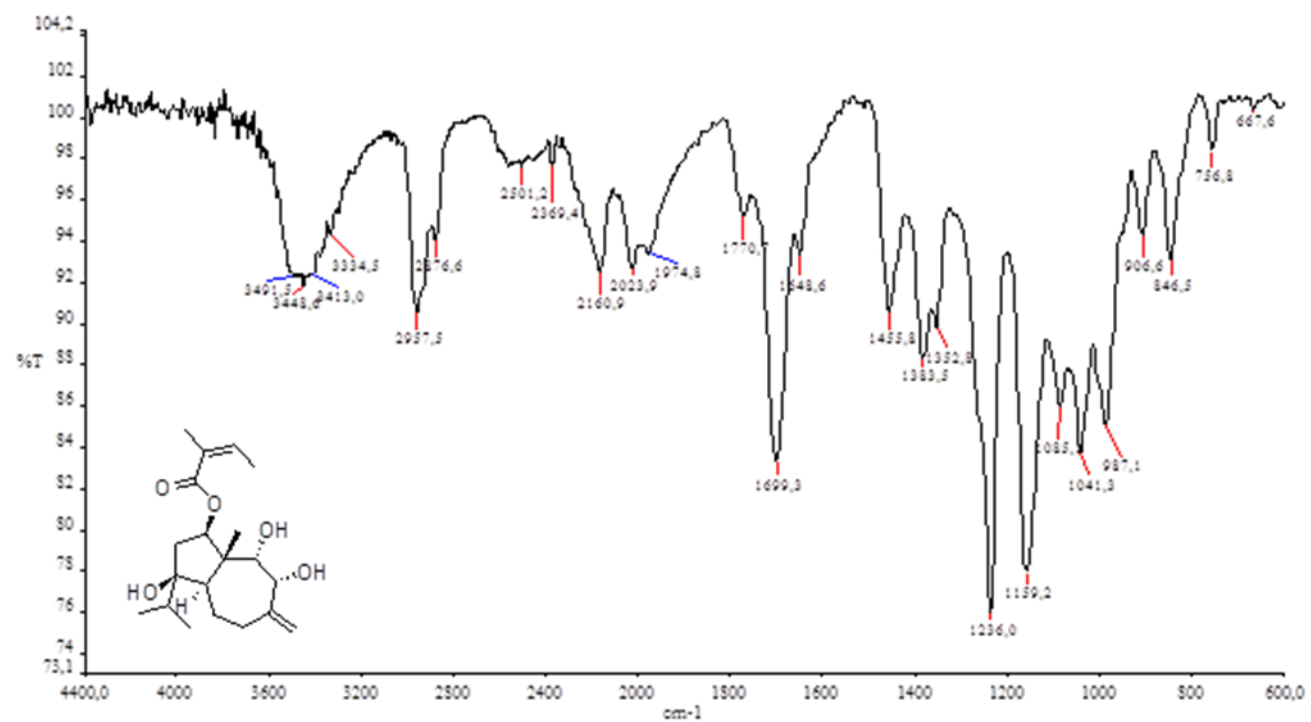
S51. HR-MS spectrum of compound **6**.



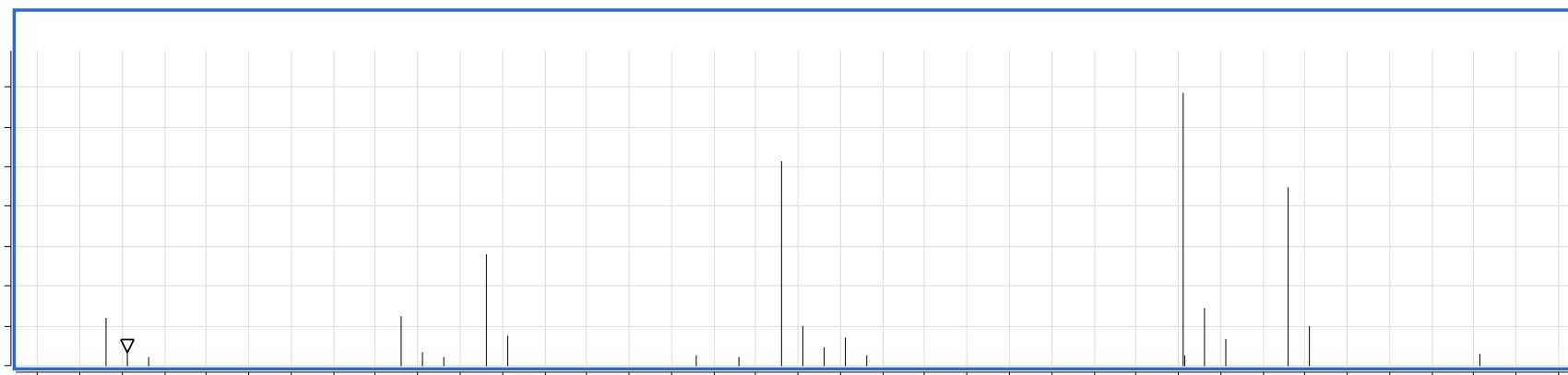
S52. LC-MS data for compound **6**. a) LC-MS chromatogram; b) Total Ion Current chromatogram; c) fragmentation spectrum of the peak of compound **6**.



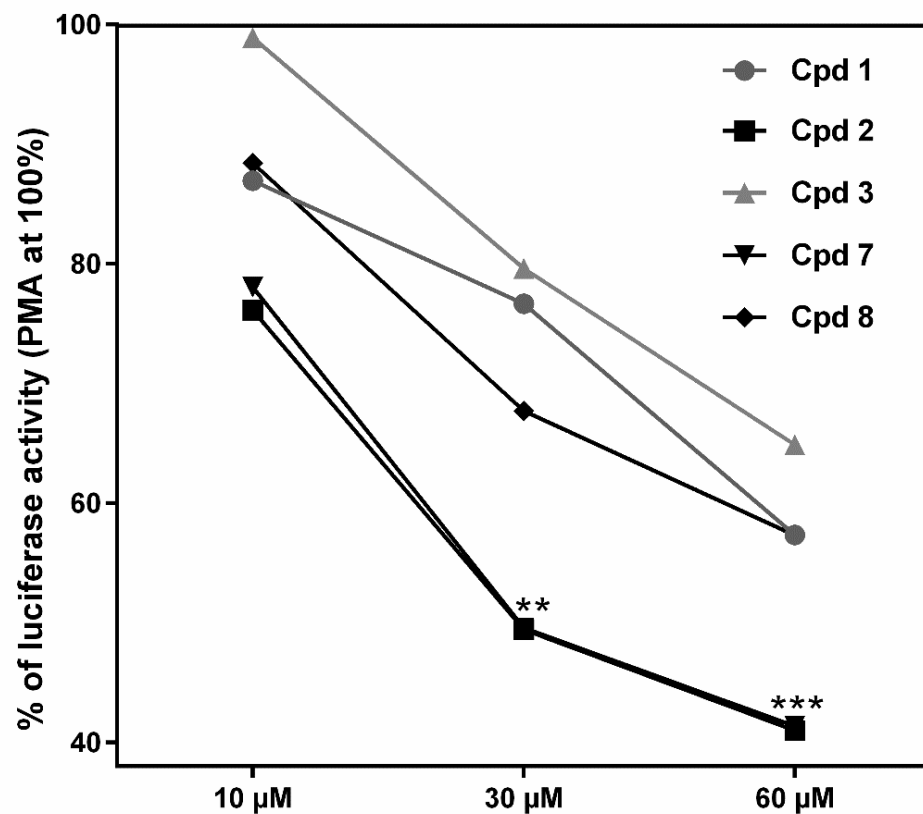
S53. IR spectrum of the compound **6**.



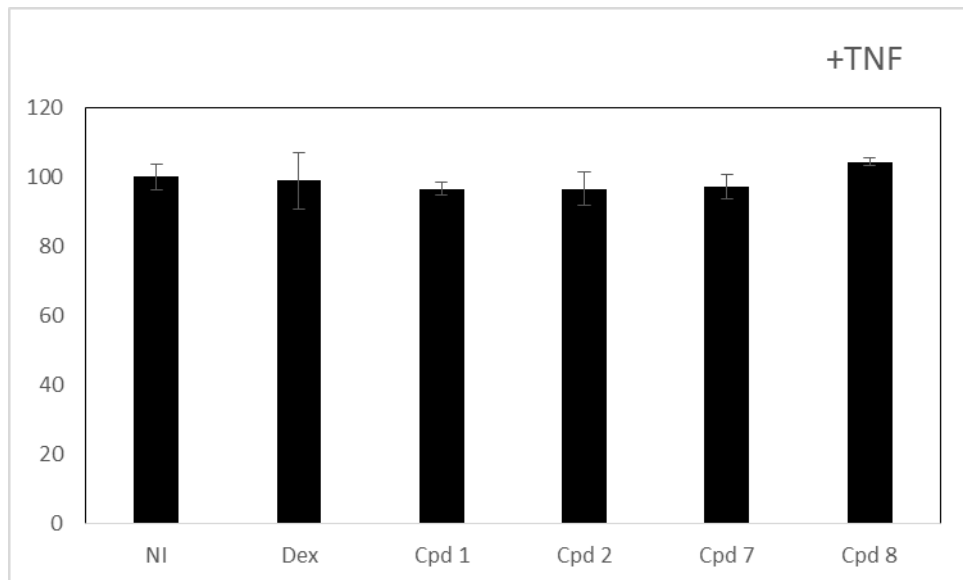
S54. HR-MS spectrum of compound **7**.



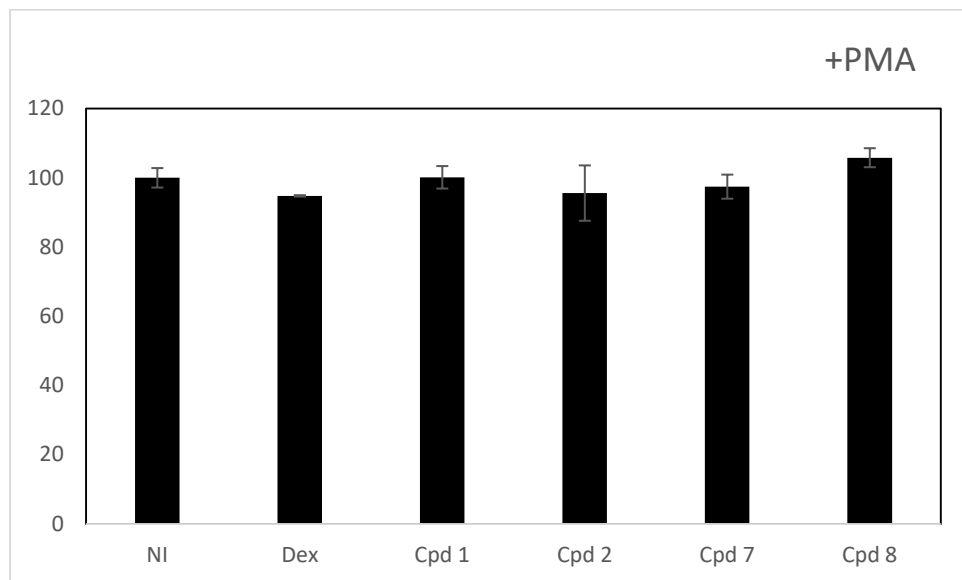
S55. Concentration-dependent effect of the five most active compounds **1-3, 7** and **8** at three concentrations (10, 30 and 60  $\mu\text{M}$ ) in PMA-induced A549 cells stably integrated with an AP-1-Luc-dependent reporter gene. Inhibition of the luciferase activity was calculated relative to the control group (solvent) treated with PMA (20 nM) being set as 100%. Dexamethasone (1  $\mu\text{M}$ ) induced a drop of activity to  $55.0 \pm 3.2\%$  (\*\* $p = 0.0019$ ). Results are shown as a mean value of four independent replicates. Statistical significance of the test results in comparison to those of the control groups were determined using one-way ANOVA (significance levels \* $p \leq 0.05$ ; \*\* $p \leq 0.01$ ; \*\*\* $p \leq 0.001$ )



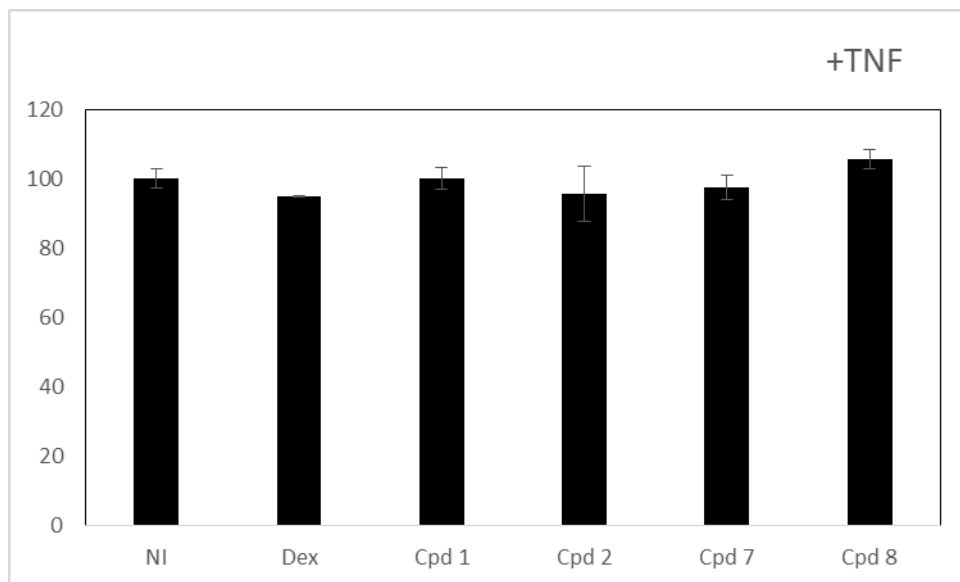
S56. Cell viability  $\kappa$ B-Luc A549 cell line as determined by the Cell Titer Glo<sup>®</sup> assay after application of compounds **1**, **2**, **7** and **8** in the concentration 30  $\mu$ M and treatment with TNF (200 IU/ml). NI-solvent control group was set as 100% of cell viability. Dex-group treated with 1 $\mu$ M of dexamethasone. Results are given as a mean value  $\pm$ SD of three independent replicates.



S57. Cell viability AP-1 Luc A549 cell line as determined by the Cell Titer Glo<sup>®</sup> assay after application of compounds **1**, **2**, **7** and **8** in the concentration 30  $\mu$ M and treatment with PMA (20 nM). NI-solvent control group was set as 100% of cell viability. Dex-group treated with 1 $\mu$ M of dexamethasone. Results are given as a mean value  $\pm$ SD of three independent replicates.



S58. Cell viability in Neo LucA549 cell line as determined in luciferase assay after application of compounds **1**, **2**, **7** and **8** in the concentration 30  $\mu\text{M}$  and treatment with (200 IU/ml). NI-solvent control group was set as 100% of cell viability. Dex-group treated with 1  $\mu\text{M}$  of dexamethasone. Results are given as a mean value  $\pm$ SD of three independent replicates.



S59. Extraction and Isolation. The aerial parts of *L. zernyi* (139.61 g) were extracted with CHCl<sub>3</sub>. After extraction, the solvent was reduced under vacuum, to obtain 4.84 g of a dark brown gummy extract. The crude CHCl<sub>3</sub> extract was re-extracted with MeOH and further separations were carried out with the MeOH-soluble fraction. Then, 3.31 g of the MeOH-soluble extract was purified on a silica gel column. Extracts were eluted with a gradient system using an increasing polarity and collecting fractions of 50 mL each: *n*-hexane-EtOAc (from 5:1 to 3:2 - 10 fractions), *n*-hexane-EtOAc (from 3:2 to pure EtOAc - 25 fractions), pure EtOAc (10 fractions), then EtOAc-MeOH (from 1:1 to pure MeOH 10 fractions) and finally with pure MeOH (7 fractions). The 62 fractions were analyzed by TLC using a molybdate salt-acid reagent for terpenoid detection, and fractions with identical composition were combined. In case of a complex mixture, an additional normal-phase separation step was done using an isocratic mobile phase flow of toluene - EtOAc (95:5) (fraction volume 5 mL). After normal-phase partitions, the fractions were subjected to preparative reversed phase HPLC using a gradient system (mobile phase composition: 0.1% HCOOH in H<sub>2</sub>O (solvent A), and CH<sub>3</sub>CN (solvent B); gradient used: 0–3 min isocratic 70% A /30% B, 3–17 min gradient 70% A /30% B to 100.0% B, 17–22 min isocratic 100% B, 22–23 min gradient 100% B to 70% A/30% B and 23–28 min isocratic 70% A /30% B). The HPLC-columns used were a Phenomenex Luna C18(2) 250x21.20 mm AXIA column and a Phenomenex Luna C18(2) 250x10 mm column, both with 5 μm particle size and used at 35°C. Depending on the different column sizes, flow rates of 4.5 mL/min or 17.5 mL/min, and injection volumes of 500 or 1000 μL were used respectively. The separation process and purity of the compounds were monitored by LC-MS (the corresponding UV and TIC chromatograms and mass spectra of the compounds are part of the Supporting Information) using a gradient system on a Phenomenex-Kinetex C18(2) column (150x4.6 mm). The mobile phase constituted of 0.1% HCOOH in H<sub>2</sub>O (solvent A), and CH<sub>3</sub>CN (solvent B). The elution program was a 0–0.5 min isocratic 70.0 % A/30.0% B, 0.5–6 min linear gradient from 70.0% A/30.0% B to 100.0% B, and 6–8 min isocratic 100% of B. The flow rate was 1.5 mL/min, the column temperature 35 °C, the injection volume 15 μL, with 214 nm as detection wavelength.

After normal-phase separation, compounds **1** and **2** were present in the fractions 18-21 (779.5 mg). A second normal phase separation of the combined fractions, followed by a final purification led to 37.8 mg of **1** and 15.6 mg of **2**. Compounds **3** and **5** were isolated from fractions 22-26 (677.9 mg) after the first normal-phase separation. Further preparative HPLC separation led to 3.1 mg of **3** and 3.2 mg of **5**. Compound **4** was isolated from fractions 44-49 (55.1 mg). Fractions were submitted to preparative HPLC separation, which yielded 6.0 mg of **4**. Compound **6** was

obtained from fractions 39-43 (12.5 mg), which were subjected directly to preparative HPLC, affording 2.0 mg of **6**. Vaginatin (**7**) was isolated from combined fractions 18-21, which were subjected to an additional normal-phase separation step, after which 11.1 mg were isolated. Laserpitin (**8**) (42.1 mg) was detected as one of the most abundant constituents in the initial extract. It was isolated from the combined fractions 22-26 after the first normal-phase separation. The subsequent preparative HPLC purification resulted in 133.0 mg of **8**.

S60. Quantification of major components of *L. zernyi* extract. In addition to isolated daucanes, the purification of some fractions allowed to characterize guaianolides of a slovanolide type, i.e. montanolide, isomontanolide, acetylmontanolide and acetylisomontanolide, and the eudesmanolide silerolide, that were isolated from the herb of *L. siler* and underground parts of *L. zernyi*, as reported previously by Milosavljević et al. (1999) and Popović et al. (2013). Using an external standard method, quantification of the terpenoids was performed in a gradient system, as reported previously by Popović et al. (2013). As the main constituents in the *L. zernyi* extract laserpitin (45.31 mg/g of extract) and montanolide (3.75 mg/g extract) were quantified. Isomontanolide, acetylisomontanolide, acetylmontanolide and silerolide were also detected, but their concentrations in *L. zernyi* extracts were too low to be precisely calculated.

S61. Cell cultures. Human A549 lung epithelial cells were purchased at ATCC (cell bank) and stably transfected with the reporter gene using a lentiviral transduction method (TronoLab, Lausanne, Switzerland). A549 cells were cultivated in DMEM (Gibco-Invitrogen, Merelbeke, Belgium) supplemented with 10% fetal calf serum (International Medical Products, Brussels, Belgium), 100 IU/mL penicillin and 0.1 mg/mL streptomycin (Sigma-Aldrich, St. Louis, MO, USA) were added to the medium. Cell cultures were maintained at 37 °C in a 5% CO<sub>2</sub> atmosphere with 95% humidity. Subconfluent cells (80%) were passaged with a solution of Gibco<sup>®</sup> Trypsin-EDTA (Gibco-Invitrogen, Merelbeke, Belgium). A549 GR-knockout cells were made by using the CrispR/cas9 knockout system via the use of GeneCopoeia (Rockville, MD, USA) vectors (ref. #CP-LVC9NU-02 and HCP208401-LVSG02-3-e). In order to obtain NeoLuc A549 for cell viability assays, basal A549 cells were stably transfected with pMet-NeoLuc and then treated for three weeks with geneticin (1 mg/mL of geneticin). For an ELISA assay, the basal A549 cells were seeded in a 6-well plate (250 000 cells/well) in medium (DMEM + 10% FCS + 1% P/S). The second day (after 24 h), a 24 h starvation was performed in wells using Opti-MEM serum (Gibco-Invitrogen, Merelbeke, Belgium). After this period, compounds (30 μM) or solvent control or dexamethasone (1 μM) were added to the wells. After the incubation of 3 h, the medium was collected and kept at -80 °C prior to experiments.